JOURNAL OF MATERIALS SCIENCE 12 (1977) 2355–2388

Review

Solid-state deformation of polyethylene and nylon and its effects on their structure and morphology

WILLIAM G. PERKINS, ROGER S. PORTER
Polymer Science and Engineering and Materials Research Laboratory, University of Massachusetts, Amherst, Massachusetts 01003, USA

Solid-state deformation processes have been used to achieve polymers of high tensile moduli. The processes are based on achieving continuity for the oriented high-strength covalent bonds of the polymer chain. This is accomplished by the pulling out of chain folds and the subsequent extension of the long polymer chains which run both through and between crystal lamellae. Three major processes are used in solid-state deformation of semicrystalline polymers. In common cold drawing, the polymer is stretched at or below the crystalline melting point. In cold extrusion, a plug of solid polymer is forced by a ram through an orifice of smaller cross-sectional area to achieve draw. The third process, hydrostatic extrusion, is similar to cold extrusion except that the solid plug is surrounded by a pressure transmitting fluid which exerts a hydrostatic pressure on the plug that forces it through an orifice. Each method has distinct advantages and disadvantages that are described. Proposed molecular models for the three solid-state deformation processes generally consider the breakup of crystalline lamellae, their orientation in the deformation direction, and the pulling out of folded chains. These unfolded chains form tie-molecules between and among the disrupted lamellae. At highest deformation, fibril formation is observed which involves the partially extended tie-molecules. It is these chain-extended tie-molecules which are responsible for the unusually high tensile properties for drawn semicrystalline thermoplastics in the orientation direction.

1. Introduction

Solid-state deformations of semicrystalline polymers can cause an efficient orientation of chains in the stress direction with a consequent large increase in mechanical properties in the orientation direction. The processing conditions for solid-state deformation vary widely with polymers. There is evidence [1, 2] that the optimum temperature for such a process lies above the so-called α transition temperature and below the crystalline melting point. This suggests that solid-state deformations are ideally done in a temperature range where the polymer crystals are able to plastically deform without the concomitant occurrence of covalent bond rupture.

The three major processes used in solid-state deformation of semicrystalline polymers are cold drawing, cold extrusion and hydrostatic extrusion. These will be reviewed later, after a general discussion on the effects of solid-state deformation on polymer structure. Because the most published work, as well as this review, deals primarily with polyethylenes and nylons, the structure and morphology of these two polymer types are discussed prior to discussion of deformation processes and the consequent products.

2. Undeformed structure and morphology

Polyethylene (both high and low density) and the various aliphatic polyamides (nylons) have been studied extensively using various solid-state deformation processes. Linear (high-density) polyethylene offers a simple hydrocarbon structure that is readily characterized and uncomplicated by side groups, labile substitutes or strong intermolecular secondary bonding forces. Its theoretical modulus is also among the highest of any thermoplastic [3]. Nylons, on the other hand, offer the promise of enhanced mechanical properties and thermal stability due to their abundant hydrogen bonding. For these reasons many laboratories, including this one, have undertaken investigations of the solid-state deformation behaviour of these two thermoplastics.

2.1. Polyethylene

2.1.1. General

Polyethylenes, $(CH_2CH_2)_n$, commonly have chain ends of methyl ($-CH_3$) or vinyl ($-CH{=}CH_2$) groups. Low-density branched polyethylene ($\rho \sim 0.91$ to $0.92\,g\,cm^{-3}$) consists of the same chain backbone but contains about 20 to 40 short (2 to 5 carbon atoms) side chains per 1000 main-chain atoms. Medium density polyethylene ($\rho \sim 0.93$ to $0.94\,g\,cm^{-3}$) contains fewer short side chains, whereas high-density (linear) polyethylene ($\rho \sim 0.95$ to $0.96\,g\,cm^{-3}$) commonly has less than 10 short side chains per 1000 main-chain atoms. Lesser concentrations of long-chain branching are also associated with short-chain branching and their effect on intrinsic viscosity and molecular weight distribution has been investigated by Billmeyer [4], Beasley [5], and Harris [6], Long-chain branching is thought to result from radical transfer from a growing chain to a dead chain, which then grows a long branch.

Polyethylenes of higher density exhibit a sharper "neck" and a greater "natural draw ratio", terms defined in Section 4.

2.1.2. Crystal structure

Polyethylene exists in a planar zigzag (2_1 helix) chain conformation and is normally found in an orthorhombic unit cell having dimensions of $a = 7.40$ Å, $b = 4.93$ Å, and $c = 2.534$ Å [7]. The projected C–C bond length in the chain backbone is 1.53 Å and the C–C–C bond angle of 112° is slightly larger than tetrahedral. A form of isomorphism exists in polyethylene in that the unit cell dimensions (and consequently the crystal density) vary with branching [8]. For example, Walter and Reding [9] found that the *a*-axis varied from 7.68 to 7.36 Å, the *b*-axis from 5.00 to 4.94 Å, and the calculated crystal density from 0.956 to $1.014\,g\,cm^{-3}$ as the branching ratio, $CH_3/1000\,CH_2$, decreased from 80 to zero. More extreme alterations of the unit cell occur upon severe sample deformations and these will be discussed in Section 3.7.

2.1.3. Spherulitic structure

Polyethylene crystallizes into spherulitic macrostructures of sufficient size to scatter visible light; thus thick specimens are opaque. This scattering originates both at the boundaries and inside of the spherulites themselves [10]. Polyethylene spherulites are negatively birefringent (greater refractive index in the tangential direction) with the molecular chain axis (*c*-axis) oriented tangentially within the spherulites. Crystal growth occurs most readily along the *b*-axis, which lies crystallographically along the radii of the spherulites. Spherulites are composed of a radiating fibrous structure and the alternating light and dark "rings" observed in many spherulites are believed to be due to a twisting of the radiating fibrils [11–14].

Spherulite size is an important factor in determining the physical and mechanical properties of polyethylene. Early detailed studies of the crystallization kinetics of linear polyethylene were conducted by Mandelkern and Quinn [15] and by Buckser and Tung [16]. They found experimentally the marked effect of temperature on crystallization rate which had earlier been predicted from theories for nucleation and growth. At greater degrees of undercooling, the spherulites are more numerous and therefore grow to a smaller size as their boundaries impinge. For crystallization nearer the melting point, fewer spherulites are nucleated, but those that are, grow larger, and the result (for a polyethylene of given branch content) is higher crystallinity for those specimens crystallized at lower degrees of undercooling. Low-density polyethylene is commonly 50 to 60% crystalline; high-density polyethylene, 65 to 90%, depending on crystallization conditions and molecular weight. Compared to most other semicrystalline polymers, polyethylene crystallizes rapidly, probably because of its regular structure, short chain repeat distance, and high chain packing density. The equilibrium melting point of a linear, high molecular weight

polyethylene was shown by Mandelkern *et al.* [17] to be near 137° C. However, under the common non-equilibrium conditions in conventional processing, the melting point is 132 to 135° C. Low-density polyethylenes melt down to 100° C.

2.1.4. Chain-folding and annealing

The underlying reasons for chain-folding in polymers have been reviewed by Lindenmeyer [18]. The driving force for folding is the lowering of conformational energy by regular (crystallographic) folding of long molecules so that van der Waals interactions come into play. Such lowering of energy by regular folding occurs only below the melting point, T_m, since at temperatures above T_m, the random coil conformation is energetically favoured [19]. Lindenmeyer [18] goes on to state that the composition of the polymer crystal will differ from that of the melt because (1) short molecules would increase the free energy of the crystal if they were incorporated, and (2) long molecules would increase the free energy of the liquid if they remain in the crystal vicinity. He therefore concludes that there is a driving force for both extremely short and extremely long molecules to diffuse away from the growing crystal. These uncrystallized entities remain as disordered regions within spherulites and at spherulitic boundaries.

Annealing of polyethylene crystals generally results in longer fold periods but, in the case of crystals with lamellae thicker than 120 Å, Keller *et al.* [20] found that the fold period decreased on annealing between 95 and 125° C. They attribute this decrease in long spacing to increased molecular tilt within the crystal lamellae. At higher temperatures, these crystals, also, thicken, and a molecular reorientation (rotation around the crystallographic *b*-axis) occurs.

During isothermal annealing, crystal thickening is usually observed to be an irreversible process, and Sanchez *et al.* [21, 22] treat the phenomenon as an irreversible thermodynamic process wherein the driving force for thickening arises from the unequal free energies of the fold and lateral surfaces. Their theory provides a basis for considering the effects of time, temperature, thermal history, pressure, and liquids on the thickening rate.

In a paper discussing temperature-induced reversible changes of long spacing in oriented polyethylene, Pope and Keller [23] conclude that large temperature-reversible changes in long spacing of polymers are a consequence of partial melting of small or imperfect lamellae leading to an increase overall periodicity. The requirement of an irregular, or imperfect crystal lattice explains why the effect is not generally observed in single crystals.

2.1.5. High pressure crystallization

The crystallization of polyethylene under pressures of 2 to 6 kbars has been investigated with regard to crystallization kinetics [24–26], morphology [24–26], and physical and mechanical properties of the resultant material [27, 28]. Two possible modes of formation of extended chain crystals under pressure are possible: (1) thickening with time of initially folded chain crystals into extended chain lamellae, or (2) direct formation from a melt of extended chain crystals. Yasuniwa *et al.* [24] believe both types of formation can occur. They postulate that the extended chain crystal grows rapidly and directly from the melt under pressure. When quenched to the crystallization temperature, T_c, of the folded chain crystal, folded chain lamellae begin to grow and thicken because extended chains have lower free energy under high pressure. These authors found no chain-extended crystals at pressures below 2500 atm. Kyotani and Kanetsuna [25] studied polyethylene crystallization at from 840 to 5300 atm and concluded that (1) isothermal crystallization occurs much faster under high pressure at comparable undercoolings, (2) the Avrami equation is valid for high-pressure crystallization and the Avrami exponent n decreases from ~2 at 840 atm to ~1 at 5100 atm, (3) the surface energy of crystal nuclei appears to decrease with increasing crystallization pressure, and (4) extended chain crystals grow at a high rate, predominantly in one dimension, under high pressure. Maeda and Kanetsuna [26] crystallized polyethylene at from 220 atm up to 6000 atm and noted three major pressure ranges. In the low range, below 2000 atm, folded chain crystals are formed; between 2000 and 3500 atm, mixed crystallization of extended and folded chain crystals takes place, while extended chain crystals become more stable and appear in larger quantity with increasing pressure; in the high-pressure region above 4700 atm, two stages of crystallization and of melting and reported, one producing "ordinary" chain-extended crystals, and the other leading to "highly extended

chain" crystals which melt at temperatures above the crystallization and melting temperatures of the "ordinary" extended chain crystals.

Early work on pressure-crystallized polyethylene was carried out by Wunderlich *et al.* [27, 28]. They found, as did Maeda *et al.* [26] ten years later, three pressure regions where folded chain, folded chain/extended chain mixtures, and extended chain crystals, grow. They also reached several additional conclusions; (1) Pressure decreases the amorphous volume more than the crystalline volume, (2) the crystallographic *a*- and *b*-axes are compressed more easily than the *c*-axis, (3) the melting point of the crystalline phase increases approximately 0.02° C atm^{-1}. and (4) the equilibrium maximum melting point of the polyethylene crystal is $140 \pm 0.5^\circ$ C. They found that at the highest pressure investigated, 5300 atm, extended chain lamellae can be as thick as 3 μm [28]. Well defined kink bands were observed in the thicker extended chain lamellae. The authors suggest that either molecular weight fractionation or an end-to-end alignment of molecules and subsequent folding takes place during the growth of the extended chain lamellae. Rees and Bassett [29] investigated the effect of pressure on the crystallization of polyethylene fractions and concluded that the thickness of extended chain lamellae is a function of time, temperature, and molecular weight. They found that crystallization is quantitatively similar to that of folded chain crystals at 1 atm, giving an optimum lamellar thickness which increases with time and decreased supercooling. These authors further noted that (1) fractional crystallization is widespread, (2) isothermal thickening of lamellae during crystallization occurs, and (3) layers can anneal to thicknesses ten times their initial size.

Extended chain high-density polyethylene has been reported by Lupton and Regester [30] to be stiffer and somewhat stronger than normal folded chain HDPE. They note that with molecular weights in the range for moulding or extrusion, the extended chain material is inductile and brittle, while molecular weights near 2×10^6 are still rigid but tough. The authors postulate a polymorphic transition between orthorhombic and triclinic phases at 5000 atm, determined from volume–temperature behaviour. Attenburrow and Bassett [31] studied the morphology of chain extended ultra-high molecular weight linear polyethylene after drawing five-fold. Crystallization is believed to proceed via a hexagonal high-pressure phase [32] into the orthorhombic crystal. The authors note that ultra-high molecular weight chain-extended polyethylene shows some ductility in tension if low molecular weight material is removed prior to pressure treatment. Because the majority of extended chain lamellae survived the drawing process, it was postulated that melting had not occurred during drawing (up to 6.5 draw ratio). However, perhaps 20% of lamellae were disrupted while others underwent uniform shearing and, as with chain-folded polyethylene, voiding and/or crazing was observed.

A review of polyethylene crystallization under pressure by Bassett [32] details a number of points: (1) chain-extended growth results from crystallization of a high-pressure hexagonal phase, (2) the hexagonal phase incorporates *gauche*, as well as *trans*, bonds along the chain, (3) lamellar thickening occurs by a local melting and recrystallization, and (4) lamellar thickness is inversely proportional to supercooling and entropy of fusion.

This discussion of polyethylene structure and morphology represents only a minute part of the extensive associated literature. Numerous important papers have been published by A. Keller, L. Mandelkern, B. Wunderlich, E. Baer, and a host of others. General reviews of polyethylene, its technology and uses, can be found in [8] and [10].

2.2. Nylon

2.2.1. Crystal structure

A second class of polymers which has been widely investigated with respect to solid-state extrusion is the polyamides, or nylons, by trademark definition, a nylon is any long-chain synthetic polymeric amide which has recurring amide groups as an integral part of the main polymer chain. Nylons are synthesized in many ways. These include the condensation of diamines with diacids, the polymerization of amino acids, and the ring-opening polymerization of lactams. The varied routes to synthesis lead to many different types of nylons whose structure and properties differ widely. The various aliphatic nylons are named by a numerical system based on the number of carbon atoms in the monomer(s) from which they are synthesized. For example:

$$H_2N(CH_2)_nNH_2 + HOOC(CH_2)_{m-2}COOH$$
$$\longrightarrow -NH(CH_2)_nNHCO(CH_2)_{m-2}CO-$$

diamine + dibasic acid ⟶ nylon *nm* + $2H_2O$

$$H_2N(CH_2)_{n-1}COOH \longrightarrow -NH(CH_2)_{n-1}CO- + H_2O$$

amino acid ⟶ nylon *m*

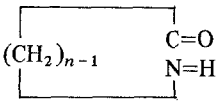

$-NH(CH_2)_{n-1}CO-$

lactam ⟶ nylon *n*

n indicates the number of carbon atoms in the diamine; *m* the number of carbons in the dibasic acid. A single number indicates the carbon number in the amino acid or lactam.

For convenience, nylons may be classified into six groups according to the number of CH_2 groups in the monomeric units [33]:

Group A; Nylons from diamines with *even* numbers of CH_2 groups and dibasic acids with *even* numbers of CH_2 groups – 66, 68, 610, 612.

Group B; Nylons from diamines with *even* numbers of CH_2 groups and dibasic acids with *odd* numbers of CH_2 groups – 49, 69, 89, 109.

Group C; Nylons from diamines with *odd* numbers of CH_2 groups and dibasic acids with *even* numbers of CH_2 groups – 76, 78, 710.

Group D; Nylons from diamines with *odd* numbers of CH_2 groups and dibasic acids with *odd* numbers of CH_2 groups – 77, 79, 99.

Group E; Nylons from ω-amino acids with *even* numbers of CH_2 groups (odd numbers in the conventional expression) – 7, 9, 11.

Group F; Nylons from ω-amino acids with *odd* numbers of CH_2 groups (even numbers in the conventional expression) – 4, 6, 8, 10, 12.

Probably the most interesting and important phenomenon common to all nylons is the presence of inter- and intramolecular hydrogen bonding. They exist in both the crystalline and noncrystalline regions. Their presence and extent is responsible for many nylon characteristics. Differences in melting temperature, water sorption, tensile properties, density and solvent resistance are found among the nylons having different concentrations of amide groups in the main chain. The crystalline melting points, for example, increase with the concentration of amide groups [34–37] as shown in Fig. 1. This is due to an increase in hydrogen bonding which increases the cohesive forces between adjacent molecules. Nylons with even numbers of CH_2 groups have higher melting points than those with odd (Fig. 1). In earlier studies it had, therefore, been suggested, on the basis of X-ray studies [38], that structures with planar zigzag chains, where hydrogen bond formation is incomplete, exist for even–odd, odd–even and odd–odd nylons [34, 35, 39]. However, it has subsequently been shown by infrared spectroscopy that hydrogen bonding between amide groups is essentially complete in both odd and even members and that no more than 1% free

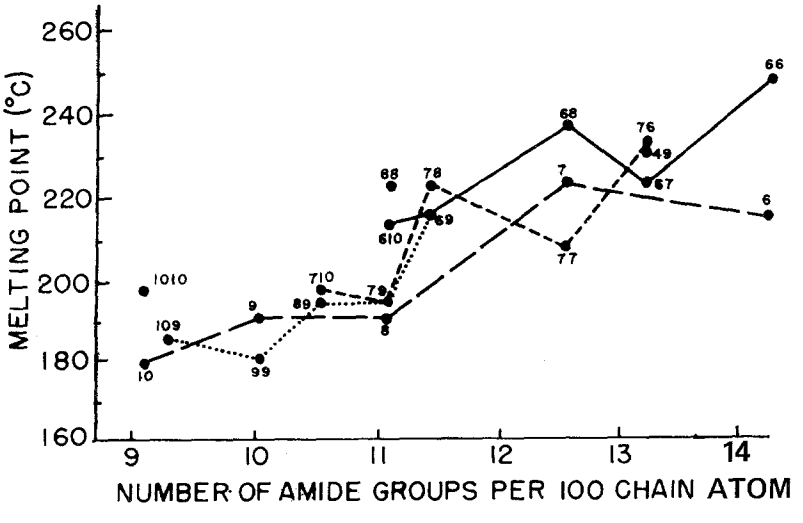

Figure 1 Melting points of polyamides; ——— from hexamethylenediamine and bibasic acids, – – – – from heptamethylenediamine and bibasic acids, ... from diamines and azelaic acid, — · — · — from ω-amino acids. (after Kinoshita [33]).

NH absorption is observable at room temperature [40]. This suggests that a structure must exist which deviates from the planar zigzag which allows essentially complete hydrogen bond formation. This structure has been called the γ-form and is the common structure for odd–even, even–odd and odd–odd nylons and sometimes occurs for even and odd nylons. The even nylons (containing odd numbers of CH_2 groups) usually exhibit the α- and β-forms for short CH_2 sequences, e.g., nylon 4 and nylon 6, while the γ-form is found in longer sequences, as nylon 8, 10 and 12.

The α-phase is comprised of planar sheets of hydrogen-bonded molecules stacked upon one another. The X-ray fibre photograph of the β-phase is characterized by a meridional spot and layer line streaks. It has been postulated that successive sheets in the β-phase are staggered "up and down" instead of always being displayed in the same direction (Fig. 2). The presence of the β-phase cannot be reliably determined except in samples possessing a high degree of axial orientation. In the γ-phase, polyamide chain bonds are rotated into a puckered or pleated conformation to form strain-free hydrogen bonds [42]. γ-phase nylons, therefore, have shorter chain-repeat distances by a nearly constant value than those calculated for the fully extended form. The γ-phase unit cells are usually pseudohexagonal [33].

Bunn and Garner [38] have shown that nylon 66 and 610 exist in both the α- and β-forms. The unit cell was found to be triclinic with one chain molecule passing through it for the α-form. An alternative packing of sheets (see above) gave a two molecule triclinic cell which is the β-form. The α-form was found to be the more stable phase. Above 165 to 175° C the unit cell of nylon 66 changes to pseudohexagonal [58, 59]. Such polymorphism is evident in the other polyamides as subsequently discussed.

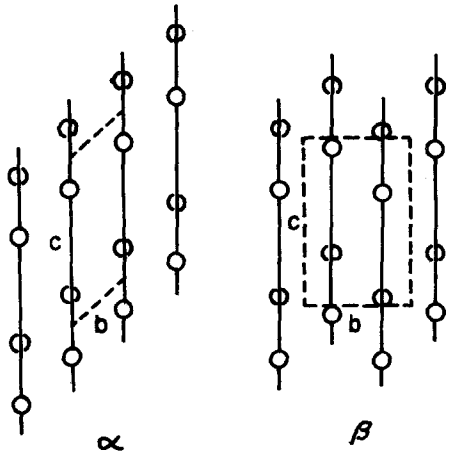

Figure 2 Arrangement of sheets of molecules in α and β crystals. Lines represent chain molecules, circles oxygen atoms. (after Bunn and Garner [38]).

The crystal structure of nylon 6 has been investigated by several authors [33, 43–48, 254] on samples of various thermal and mechanical treatments. The α-, β- and γ-forms have all been postulated. It has been concluded [33, 43, 48] that the α-form is the most stable and the β-form can be converted to the α-form by immersion in boiling water for 5 or 6 h [43]. The shifting of the hydrogen bonds generates the different crystalline forms [48], e.g. the α-form which is characterized by sheets of antiparallel chains [33, 46, 47] with the structures being interconvertible [47, 52–57]. The α-form can be converted to the γ-form by treatment with an aqueous I_2–KI solution and an aqueous solium thiosulphate solution, while the γ-form is convertible to the α-form by treatment with aqueous phenol or by stretching at high temperature [47, 52–57]. Lindenmeyer [254] has observed stable α and γ crystals in highly annealed nylon 6 fibres. Metastable pseudohexagonal crystals were also observed.

Recently, a method has been developed [60, 61] relating quantitative structural information to wide-angle X-ray diffraction results, using nylon 6.

The structure of nylon 11 has been studied by various researchers [33, 62–66]. The unit cell is triclinic, having diameters $a = 4.9$ Å, $b = 5.4$ Å, $c = 14.9$ Å; $\alpha = 49°$, $\beta = 77°$, $\gamma = 63°$ [62]. Slichter [63] found that, for nylon 66 and 610, the lateral asymmetric packing in the basal plane of the triclinic cell shifts towards hexagonal packing as the temperature is raised. A concomitant shortening of unit cell length was attributed to twisting of the chain segments during motion. Similar polymorphism has been noted in nylon 11 [64, 65]. Genas [64] found that, above 70° C, the *a*, *b* (basal) plane of the triclinic cell assumes hexagonal packing. Onogi *et al.* [65], found that quenched film of nylon 11 contains γ (pseudohexagonal) crystals, while film solution cast from *m*-cresol contains α (triclinic) crystals. When films containing γ crystals were annealed above 90° C, they transformed into the α modification.

The structure of nylon 12 has only recently been investigated [49, 50]. It exhibits [50, 51] the γ-phase (Fig. 3). Northolt *et al.* [49] also

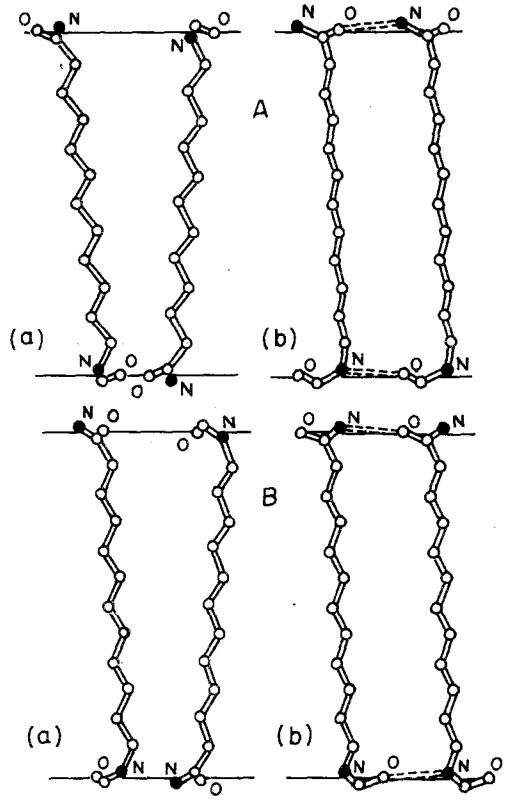

Figure 3 (A) Crystal structure A of the γ form of nylon 12 (a) projection on the *ab* plane (b) projection on the plane perpendicular to the *a*-axis. (B) Crystal structure B of the γ form of nylon 12 (a) projection on the *ab* plane (b) projection on the plane perpendicular to the *a*-axis. (after Inoue and Hoshino [50]).

found that nylon 12 may exist in two different forms, depending on conditions. Melt-pressed sheet that was quenched in ice water, drawn 4.5 ×, and annealed at 170° C at constant length for several hours under nitrogen, revealed a hexagonal unit cell, while melt-pressed sheet that was quenched in ice water, drawn 7 ×, and cooled under stress to room temperature, exhibited what appeared to be a mixture of mono- and triclinic unit cell structures. Inoue and Hoshino [50] prepared their sample by drawing a nylon 12 monofilament 3.6 × in boiling water then annealing it at 150° C for 10 h. They found a monoclinic unit cell resembling the γ-form of the other even nylons. No transition to the α-form was observed even when the sample was subjected to stretching at temperatures near 150° C or treated with aqueous phenol. It was, therefore, decided that the γ-form of nylon 12 is more stable than for nylon 6, nylon 8 or nylon 10. This led to the conclusion that the longer the molecular chain in the even nylons, the more the crystal shows a tendency to form the γ-phase. Ishikawa *et al.* [51] used sheets drawn from 2.4 to 4.0 × at from 50 to 150° C, they also detected the γ-form under all test conditions.

2.2.2. Morphology

Most studies of polyamide morphology have been on nylon 66 [67–74]. Many aspects of its structure and behaviour apply to other nylons.

Like most semicrystalline polymers, nylons normally crystallize in spherulitic forms. Under mechanical stresses or strong thermal gradients, most crystalline polymers show a variety of non-spherulitic and oriented structures. Nylons, however, under usual processing conditions, yield spherulitic forms. Kohan [42] believes this is because the melts tend to supercool markedly. He feels that by the time crystallization begins, the stresses have reduced greatly from the initial values and the environment approaches a quiescent condition. This could also be responsible for the apparent absence of spherulites in crystalline nylon samples which have a milky appearance. The spherulites are, in fact, present, and scatter visible light, but are too small to be seen with a light microscope.

The many studies of nylon 66 [67, 73, 74, 78–80] have revealed the formation of four types of spherulites under different conditions, these are:

(1) Positive spherulites; These are spherulites having their larger refractive index in the radial direction. They grow exclusively when the melt is cooled rapdily to below 250° C. They can also grow at higher temperatures in combination with other forms. Experimental data from infrared spectroscopy [72, 81], X-ray diffraction [78] and electron microscopy [79] suggest that positive spherulites are composed of fine fibrils of folded chain ribbons. The planes of the hydrogen bonds (*a*-axes) are directed along the radii.

(2) Negative spherulites; These are spherulites having their larger refractive index in the tangential direction. These grow between 250 and 270° C and are always accompanied by spherulitic aggregates. These spherulites grow faster than positive spherulites and, as shown by X-ray [78], are highly crystalline but with little preferred orientation of the unit cells. Infrared data [73] indicate well developed chain-folding comparable with that in single crystals. Negative spherulites seem to be composed of lamellae type crystal units rather

than the branched fibrils formed in positive spherulites.

(3) Nonbirefringent spherulites; These occur in two temperature ranges. One is around 250° C, the other is around 265° C. No evidence of any preferred orientation of the unit cells has been found in these spherulites. It has been suggested [82] that this type of spherulite results from a mixture of positive and negative types.

(4) Spherulitic aggregates; Found with negative spherulites but grow faster. They show evidence that the crystallographic *b*-axis is parallel to the radius although this orientation varies with location. They are strongly birefringent.

Starkweather and Brooks [68] investigated the effect of spherulites on the mechanical properties of nylon 66. They found that spherulite size was important in dry samples at low temperatures (23° C) and becomes less important with increasing moisture content and/or temperature. Dry samples with smaller spherulites show higher flexural modulus, a higher yield stress, and a lower ultimate elongation than samples with larger spherulites. As spherulite size decreases, the yield point increases (Fig. 4). The yield points of spherulitic films are substantially higher than those without visible spherulites, independent of the crystallinity [67].

The rate of nylon crystallization depends partly on composition, thermal history and the presence of nucleating or plasticizing additives [42]. According to Kohan, the amide concentration and

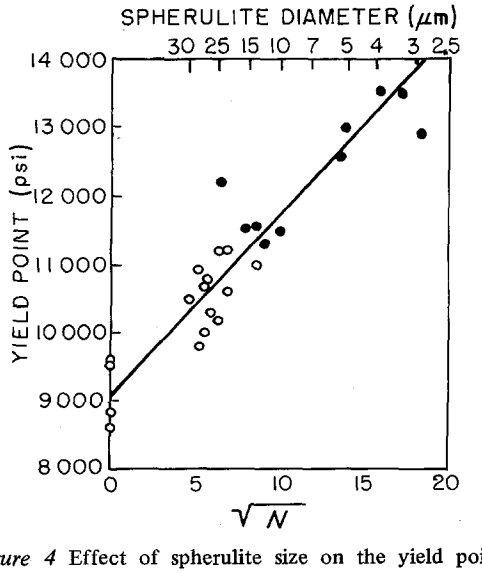

Figure 4 Effect of spherulite size on the yield point: compression-moulded films ○; injection-moulded bars ●. *N* is the number of spherulite boundaries per millimeter. (after Starkweather and Brooks [68]).

molecular symmetry are important. For a given class of nylons, the rate of crystallization will typically rise with increasing amide concentration at constant undercooling. At a given amide concentration the series with the highest degree of symmetry (e.g., even–even) will have the highest rate of crystallization. The more rapidly crystallizing nylons are generally the higher melting.

An increase in either the melt temperature or time in the melt will lower the crystallization rate. The influence is on both the induction time for crystallization and on subsequent growth rate. This implies that the melt has a memory [42].

Added agents can effectively nucleate crystallization rates and increase amounts. Such materials are commonly (1) solid near the melting point of the nylon, (2) finely divided, (3) do not agglomerate, and (4) provide polar surfaces capable of adsorbing amide groups. Effective agents including sodium phenylphosphinate, sodium isobutylphosphinate, magnesium oxide, mercuric bromide and chloride, cadmium and lead acetate, and phenolphthalein as well as silver halides and fine silicas and aluminas [84].

The infrared technique for identification of chain-folds [72] indicates that folding in melt-crystallized samples of nylon 66 is the same as in single crystals prepared from solution. Samples which are initially quenched to low crystallinity show no regular folding, but regular folds are formed on annealing. Additional infrared studies [73] show that the regularity of chain-folding is related to the type of spherulitic growth.

Moisture increases the rate of crystallization due to a plasticizing action which increases chain mobility [83], but in practice water is avoided because it leads to degradation and bubbles.

The change from dryness to water saturation causes a fourfold decrease in modulus of oriented nylon 66 in the machine direction at room temperature (Fig. 5) while the principle mechanical relaxation, the glass transition, is shifted downward by about 70° C [71].

Moisture also has a large effect on the morphology and thus the properties of polyamides. It is believed [70] that only the disordered portions of the polymer are accessible to water. This may be due to strained, metastable, hydrogen bonds present in the chain folds and other noncrystalline regions which are disrupted and reformed in conjunction with water molecules. Although nylon is more dense than water, its density increases as

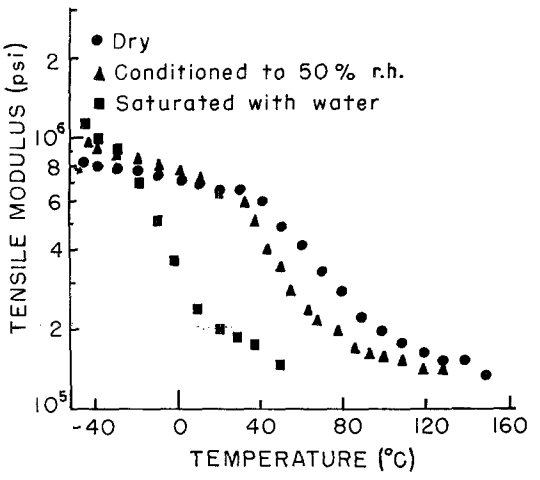

Figure 5 Tensile modulus of oriented nylon in the machine direction. (after Starkweather [71]).

water is absorbed, up to about 2.5% [70]. This again is apparently due to disruption of strained hydrogen bonds which allows the hydrocarbon chain units to pack more closely, thus decreasing the volume. On the other hand, the water molecules could just be filling in intermolecular spaces in the amorphous regions. An early review of the sorption of water by polymers, including thermodynamic theories, was written by McLaren and Rowen [85]. They showed how both solution theories and sorption theories are useful in predicting observed vapour pressure–water uptake relationships.

In oriented nylons, water has less effect on properties in the transverse direction than in the orientation direction. The hydrogen bonding takes place in the transverse direction between chains. One may, therefore, surmise that many of the hydrogen bonds, presumably those in the more ordered (crystalline) regions, are little affected by the absorbed water.

One last aspect of nylon morphology is the effect of high crystallization pressures. Gogolewski and Pennings [86, 87] studied the crystallization of nylon 6 from the melt under elevated pressures. Although the effect of water content was not systematically investigated, they noted no difference in high pressure crystallization behaviour between samples exposed to laboratory humidity and samples kept in a vacuum desiccator over P_2O_5. Some other results were: (1) caprolactam (monomer) molecules stabilize the chain-folds and therefore diminish the effect of pressure, (2) a pressure of 5 kbars is necessary for chain-extended nylon 6 molecules to form (~3 kbars is sufficient to form extended chain polyethylene), (3) the melting point of nylon 6 crystallized for 320 h at 315° C and 8 kbars was 256° C (41° above chain-folded nylon 6) and the authors believe it would increase further if more caprolactam had been removed from the system. A one-stage process for the development of extended chain crystals of nylon 6 was postulated from the results of these investigations.

The process of solid-state deformation involves a permanent conformational change of polymer molecules as contrasted with the temporary translation of chains occurring in melt processing. This change, in some cases, alters the basic unit cell structure, and, in virtually all cases, significantly alters the physical and mechanical properties of the deformed polymer. For semicrystalline polymers, the solid-state processing should take place under conditions where the polymer crystals will plastically deform without rupturing. This usually means that the deformation will optimally be done at or above the so-called α (crystal–crystal) transition temperature at relatively slow rates. The changes undergone by polymer crystals and associated amorphous regions are described in the following section.

3. Effects of deformation

3.1. Crystallinity

Fibre-forming polymers, as a rule, can be partially crystallized. Most are initially partly crystalline with the crystallinity being increased by deformation. The increase depends on the shape and arrangement of the macromolecules. Crystallites mainly form due to intermolecular bonding originating from the mutual attraction forces among macromolecule groups [88]. The magnitude of these forces depends on the amount and strength of the active groups, and the ability of such groups to approach each other. The greater the forces arising between the groups in neighbouring molecules, the more groups available, the more regular their disposition along the chain, and the closer to one another these macromolecules can get, the stronger are the intermolecular bonds, resulting in more facile polymer crystallization [88].

Orientation involves molecular arrangements in both crystalline and in amorphous regions. The higher the orientation, the more mutually parallel are the molecules, and the smaller is the average angle formed by them with the fibre axis. The

process of axial orientation increases crystallinity by both orienting the molecules and by bringing them closer together, enabling crystallites to form from formerly amorphous regions. As with polyethylene [89, 92] a slight increase in crystallinity with drawing is generally observed. In one case for polyethylene [90], a decrease in crystallinity was observed for annealed film at low draw ratios and a subsequent increase on further drawing. The initial decrease was reportedly due to two phenomena: (1) the crystals of a fibre structure exhibit larger paracrystalline disorder [91] and (2) the decrease of long period, due to the destruction of spherulites preceding fibril formation, increases the surface-to-volume ratio and hence reduces the density.

For nylon 6 [93], fibre crystallinity was shown to increase 27% on drawing 375% (3.75 x). Stretching took place in air at 50 cm min^{-1} at 20° C and 60% r.h. A corresponding increase in crystalline size (both parallel and perpendicular to the drawing direction) was also noted. Upon further stretching to 4.5 x, both percent crystallinity and crystallite size (in both directions) diminished. This was reportedly due to the emergence of high stresses at the greatest draw ratios, causing the destruction of some crystallite regions with imperfect or partially disturbed lattices. Prevorsek and Sharma [94] found that the drawing of nylon 6 caused little effect on crystallite size in the direction of orientation, while the crystallite width decreased with draw.

3.2. Structural models

Prevorsek *et al.* [95, 96] proposed that drawn nylon 6 is composed of microfibrils having dense crystalline parts and less dense "non-crystalline" parts, surrounded by a matrix of intermediate density. They further concluded that the microfibrils slip past one another during stretching, on the basis of three experimental facts [95]: (1) the longitudinal structure of the microfibril (amorphous and crystalline lengths) remains essentially unchanged, (2) the microfibril thinning exceeds that of the fibre, (3) the spacing between the microfibrils increases. The authors feel that in the drawing process the microfibrils are sheared with respect to each other and the matter removed from the surfaces of the microfibrils forms an interfibrillar phase whose density is similar to the average density of the microfibril. Consistent with these results, a model was proposed [95] where

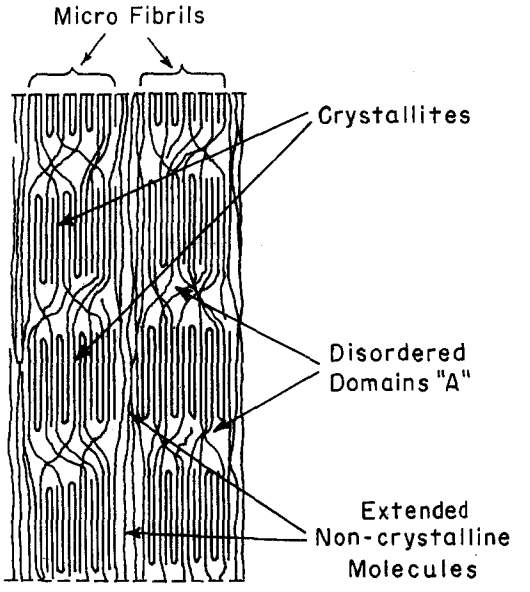

Figure 6 Structural model of nylon 6 fibres (fibre axis vertical). (after Prevorsek *et al.* [95]).

the microfibrils are embedded in a paracrystalline matrix (Fig. 6). According to Prevorsek, this differs from the model proposed by Peterlin [97–100] and others [101–102] who worked mostly with polyethylene, which assumes that the strongest element of the fibre is the microfibril. This microfibril consists of highly oriented folded chain crystals which are connected by many tie-molecules within the amorphous layers separating the crystals (Fig. 7). These authors [97–102] attribute the increase in fibre strength with increasing draw ratio primarily to the increase in the number of tie-molecules which allegedly increases the strength [103].

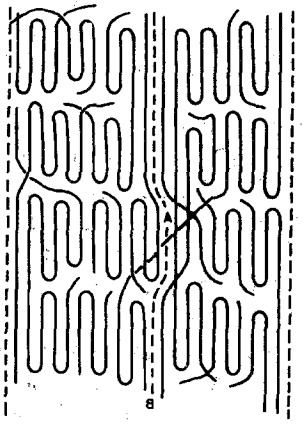

Figure 7 Microfibrillar model of fibre structure: interfibrillar (A), intrafibrillar (B) tie molecule. (after Peterlin [98]).

Prevorsek *et al.* [95, 96], however, conclude that the microfibril structure, and thus its strength, remains essentially unchanged during drawing. They feel that the increase in strength on drawing must be attributed to the transformation of the (weak) microfibrils into a strong, highly ordered, noncrystalline intermicrofibrillar phase. Their analysis of molecular dependence of fibre strength suggests that this intermicrofibrillar phase consists of highly extended polymer chains [104], and that this is responsible for fibre properties such as strength, modulus, and diffusion of small molecules into the fibre. The relatively weak microfibrils are thought to be mainly responsible for the dimensional stability of the fibre. This description is known as the "Swiss Cheese" model [95].

Actually, the Peterlin and Prevorsek models are quite similar since Peterlin also postulates that some of the tie-molecules run laterally between microfibrils and are subsequently extended as the microfibrils initially slide past one another [100]. Therefore, the strength of his model derives from these *inter*fibrillar tie-molecules, as well as from the *intra*fibrillar tie-molecules (see Fig. 7). According to Peterlin [89], the folded chains in the microfibrils are responsible for the periodicity observed from X-ray diffraction, while the partially extended tie-molecules provide the strength. He proposes [105] that the stress concentration on the tie-molecules varies throughout the sample due to length variations. Therefore, the most highly strained chains become taut and fail long before the sample breaks. As these strained chains rupture, sample weakening proceeds until, finally, microcracks develop and lead to final fracture of the fibre. This microcrack phenomenon is indeed observed during the tensile testing of many polymers including both high-density polyethylene and nylon 12 fibres studied in this laboratory.

The basis for the Peterlin model for polyethylene is a two-step deformation process [106]: destruction of the original microspherulitic structure and deformation of a new fibre structure. Tilting and slipping of lamellae initiates the first mechanism, and the resultant folded chain blocks are incorporated into well aligned microfibrils which are held together by tie-molecules. Although destruction of the spherulitic morphology is nearly completed at a draw ratio of about 10, tie-molecule content increases up to a draw ratio of about 20 [107] due to a pulling out of molecules from the folded chain blocks. Plots of modulus versus draw ratio (DR) [107] show a steep increase in modulus from DR: 10 to DR: 20 supporting this contention.

Fracture of drawn semicrystalline polymers is seen [108] as originating at point vacancy defects caused by the ends of microfibrils incorporated into the microfibrillar superlattice. Cracks then propagate radially and axially from these defects. Because axial crack growth involves the rupturing of fewer tie-molecules, it is likely to be favoured, causing the fibrous fracture surface commonly seen in stress/strain curves of such materials [109]. Peterlin [110] postulates that sliding of the fibrils during stretching does not affect the morphology of the microfibrils but rather heals the aforementioned point vacancy defects. This causes a more perfect lateral contact between fibrils and results in a steadily increasing resistance to plastic deformation. He notes [109] that over long molecular distances, van der Waals forces will effectively act to retard plastic deformation (once the fibrous structure is formed) of microfibrils and cause the observed strain hardening effect as well as increase the elastic modulus and breaking stress as the draw ratio increases. Peterlin [111] also notes that the fracture surface of drawn nylon 6 is not fibrillar and surmises that the lateral cohesion of the microfibrils in polyamides, being much stronger than in polyethylene, makes it easier for the crack to grow radially than axially although longitudinal microcracks are observed at high magnification. Peterlin further proposes that necking and post-neck deformation are separate processes for polyamides. A two-stage drawing process is indeed the method employed by Barham and Keller [112] for producing highly drawn nylon 66 (and also by Clark and Scott for polyoxymethylene [2]). Another aspect of polyamide deformation is the important role of *inter*fibrillar tie molecules, formed by shear displacement of microfibrils, which may have a greater effect on the mechanical properties of the drawn structure than the originally prevailing *intra*fibrillar tie molecules. Finally, Peterlin [111] postulates that drawing of polymers with a liquid crystal structure yields a highly aligned fibrous structure with very few chain folds and an exceptionally high tensile modulus and strength. However, the small fraction of axially oriented tie-molecules prevents the modulus from approaching that of a perfect crystal.

Takayanagi and Kajiyama [113] propose a model for drawn, crystalline polymers wherein the

dominant mechanism of deformation at lower temperatures is the breakdown of lamellar crystals into mosaic blocks. They propose that the α relaxation in bulk crystallized polyethylene can be separated into an α_2 absorption, associated with shear deformation of lamellar crystals, and an α_1 absorption, corresponding to molecular motions in the region of intermosaic blocks. The latter is presumed to contain tie-molecules much as in the Peterlin model. Also consistent with Peterlin [106], Takayanagi and Kajiyama believe that the mosaic blocks are not locally melted during deformation. These authors also investigated the effect of uniaxial compression on a highly-oriented solid-state extrudate. Kink bands were visible and small-angle X-ray scattering (SAXS) measurements indicated a thinning of lamellae crystals, caused by tilting (α_2 mechanism), in the kink bands. By using wide-angle X-ray scattering (WAXS) to correlate the tilting of molecular chains in the crystal and the alignment of crystallites in the ripple,* the authors concluded that the deformation was achieved by both the α_1 and α_2 mechanism. They further postulate that the relative contribution of the α_1 or α_2 mechanisms to the total deformation depends on temperature.

Another model considers essentially complete crystallization but with many vacancies and dislocations within the lattice. This model was proposed for nylons 66 and 610 in an early work by Zaukelies [114]. The theory was based on observations of crystallographic kinking on compression of nylon samples. Such kinking allegedly involves crystalline slip. This slip is seen as beginning at screw and edge dislocations as well as at vacancies resulting from chain ends and chain folds within the (paracrystalline) lattice. Zaukelies supported this theory with density, WAXS, and diffusion phenomena. This general idea of paracrystalline structure for semicrystalline polymers has been detailed and supported by Hosemann in a lengthy review [115], with his original ideas published in 1950 [116]. Hosemann envisions a paracrystalline superstructure incorporating aspects of both the fringed micelle and folded chain theories. Kinks, jogs, caterpillars, and other specific conformations which are found in polyethylene [117–119] are seen as distorting the crystal lattice and breaking down long range order. Behaviour of polyethylene subjected to irradiation, nitric acid etching, annealing, and stretching, as well as X-ray diffraction and NMR have been offered in support of the theory.

Point *et al.* [120] investigated the effects of rolling deformation on nylon 11 by SAXS and WAXS. They concluded that the deformation of both superlattice and subcell can be accounted for by a sliding displacement along consecutive hydrogen bonded planes. They postulate a model wherein the sample consists of parallel arrays of crystalline and amorphous layers which are thought to deform equally, while the number of lamellae in a stack remains constant.

Deformation by rolling of nylon 11 was also carried out by Gezovich and Geil [121], who found that the chain axes gradually tilt toward the rolling direction. As deformation increased, WAXS reflections broaden indicating a partial breakup of crystallites. Thus, the state of nylon 11 at high deformations was shown to be many small crystallites with a high degree of orientation.

A review by Bowden and Young [122] encompasses the broad array of crystalline polymer deformation processes occurring at modest strains. These authors note that polymer crystals can deform plastically by slip, twinning, and by martensitic (shear) transformations, and that slip produces the largest plastic strains. They show that slip in the chain direction can be either "fine", where the crystal surface normal rotates with respect to the chain direction, or "coarse" (interfibrillar) slip where the crystal surface normal remains parallel to the chain axis and lamellae are sheared with respect to one another, see Fig. 8. Two other modes of polymer crystal deformation recounted are transverse slip and twinning. Transverse slip involves the sliding of molecules over each other perpendicular to the molecular axis. Twinning is a rotation of the crystal lattice (to a greater extent than by slip) and commonly occurs in polyethylene deformation and to a lesser extent in the nylons. The authors [122] also review deformations of the amorphous phase of semicrystalline polymers. Three important modes are listed as:

(1) Interlamellar slip, where lamellar crystals are sheared parallel to each other with the amorphous phase undergoing shear.

(2) Interlamellar separation, involving a stretching of the amorphous phase between lamellae, and

*A lamellar laminate indicating crystallite alignment; essentially parallel to the edge of the kink band.

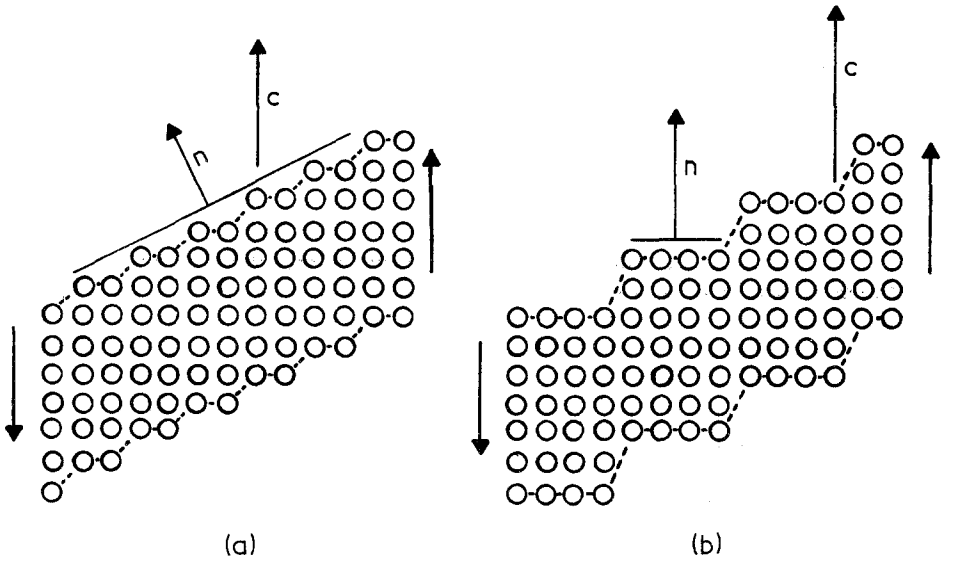

Figure 8 Schematic diagrams of crystal slip. (a) Fine slip; A displacement of one lattice vector has occurred on every other lattice plane in the crystal. (b) Coarse slip; The same total shear has been produced by a displacement of two lattice vectors on every fourth plane. The direction n is the normal to the surface of the crystal which has rotated relative to the chain axis c during deformation. (after Bowden and Young [122]).

(3) Stack rotation, which assumes that lamellae are free to rotate under stresses and are surrounded by amorphous material which distorts under deformation.

Keller and coworkers [123] have developed a structural model based on their observations of self-hardening of linear polyethylene fibres. They found that highly drawn samples, held at fixed length, relax at elevated temperatures with a concomitant decrease in modulus. However, when held for long times at room temperature, the modulus (and density) increased substantially. The authors propose a model wherein needle crystals are aligned in an amorphous matrix. During heating, stressed tie-molecules detach from the needle crystals and subsequently recrystallize in the usual chain-folded manner. However, the fibrous (needle) crystals determine their (folded chain crystals) orientation analogously to shish-kebab and row-nucleated structures. This model explains the observed drop in modulus, the persistence of X-ray orientations, the increase in lamellar content, and the absence of large contractions in subsequent reheating of these "aged" fibres. The self-hardening is explained in their model by a stiffening of the matrix [123].

3.3. Spherulitic deformation

In order to fully investigate the effects of solid-state deformation on semicrystalline polymers, one must examine what happens to the spherulitic structure during deformation. Hay and Keller [124] published a lengthy review of spherulitic deformation, using polarized light microscopy, X-ray diffraction, and electron microscopy and using high-density polyethylene film as starting material. They noted two types of spherulitic deformation during tensile drawing; homogeneous and inhomogeneous. In homogeneous deformation, all parts of a given spherulite extend simultaneously and in proportion while in inhomogeneous deformation, the spherulites and/or regions between them, yield selectively in areas that draw out fully, the rest of the microstructure remaining unaltered. Further stretching occurs by the drawn-out regions spreading at the expense of unaltered regions. Most observed cases, they submit, are intermediate between the two types. These authors [124] also note that often the deformation within a spherulite is greater than that in the material between spherulites, reflecting a weakness within the spherulites themselves. Some other observations were: (1) The formation of cracks parallel to the draw direction, with the resulting fibril widths corresponding to the deformed spherulite widths. (2) That spherulite deformations are not affine. (3) That crystallite and spherulite deformation are related but not simply. (4) The greater the deformation, the greater the c-axis alignment, and (5) chain-folding occurs even in highly drawn structures [124].

Many other authors [125–131] have studied the deformation of spherulites in terms of the microstructure. Among these, Stein, in particular, has pioneered in the development of experimental methods [132–136]. Working mostly with low density polyethylene, he has found [137] that, although the overall spherulite length on stretching may parallel the change in sample dimensions, the microdeformation may not. Often, the spherulite is found to deform more near its equator than elsewhere [124, 138]. This gives rise to a density depletion in this part of the spherulite, possibly associated with the formation and propagation of microvoids between separating lamellae [137]. Such deformation processes are also rate dependent, i.e. a finite time is required for crystal orientational changes. Thus, if a polymer is stretched at a high rate, so that crystal orientation lags behind strain, large strains will concentrate on intercrystalline tie-chains, and tend to make the polymer brittle. However, if the polymer is stretched slowly, the strain will be more evenly distributed over the sample, due to conformational changes, which then may deform in a more ductile manner. The rate of structural response and the resulting mechanical properties depend upon the size, perfection, and organization of the crystalline and amorphous regions [137].

Samuels has also performed numerous investigations of spherulite deformation [139]. Working mostly with isotactic polypropylene, he used small-angle light scattering (SALS) to follow spherulite deformation and orientation [140, 141]. Isotropic light scattering equations were extended to include the anisotropy of polarizability and the change in shape of the spherulite deformed under uniaxial tension [140]. By relating the molecular orientation of the crystalline region (the crystalline orientation function, f_c) to the gross sample deformation, the spherulites were shown to be deformed affinely [140]. In addition, quantitative information about the size of the original, undeformed spherulites and the deformed spherulites, was gained by SALS. Results from spherulitic isotactic polypropylene films drawn at 110° C may be summarized [139]: (1) all films contained negatively birefringent spherulites with the *a*-axis of the lamellae parallel to the radial direction, (2) along the radii aligned parallel to the extension direction, disruption and realignment of the lamellae occur in the inner regions of the spherulite whereas little or no change occurs in the outer regions, (3) the lamellae aligned along radii in the region of the spherulite transverse to the deformation direction undergo two processes: (a) lamellar slip leading to *c*-axis orientation, and (b) separation of lamellae. This increasing *c*-axis orientation continues until the lamellae become fully aligned, at which point crystal cleavage begins. In this highly extended state, the substructure is no longer spherulitic but fibrillar. To accommodate further extension, the lamellae cleave and break off in blocks and the helical axis of the noncrystalline molecules becomes more oriented in the deformation direction [139]. Similar films drawn at 135° C behave in a like manner, except that the lamellae are larger, more perfect, and thus less deformable, and the noncrystalline molecules are more mobile. This leads to diminished internal disruption within the spherulite during extension, since relaxation processes occurring within the noncrystalline region result in deformation processes that are non-orienting in character [139].

Other investigations involving isotactic polypropylene fibres and poly(ethylene terephthalate) yarns are detailed in [139].

The spherulitic deformation of nylon 66 has been investigated by Crystal and Hanson [142] using optical microscopy, electron microscopy, and small-angle X-ray scattering. They found that spherulites elongated into football shapes along the draw direction when drawn 4 x. This indicates that spherulite deformation is symmetric about a central axis parallel to the draw direction. Sample density also decreased upon cold drawing. This is consistent with Stein's contention [137] that microvoids are formed by non-uniform spherulitic deformation. The fibrils of impinging spherulites run together and intertwined over a width of 0.5 to 0.8 μm, forming a diffuse boundary containing fibrils from multiple spherulites. The spherulite elongation was less than $\frac{1}{2}$ the sample elongation, indicating that the spherulites slipped with respect to each other, and the fibrils parallel to the draw apparently became thinner, while those perpendicular to the draw became thicker. Fibrils at intermediate orientations were bent toward the draw direction.

A study of the deformation of nylon 6 spherulites under uniaxial stretching was done by Matsuo *et al.* [143]. X-ray diffraction and SALS were used. The model proposed was similar to that for the deformation of low density polyethylene [144]. The spherulitic deformation is accepted as

occurring in two steps: "instantaneous" deformation of the spherulite, associated with orientation of lamellar axes and untwisting of crystal lamellae, and reorientation of crystallites within the oriented lamellae after a time-lag, as shown by Stein and co-workers. The authors [144] propose a model wherein the uniaxial deformation of polyethylene spherulites is discussed on the basis of an orientation distribution function of crystallites within the crystal lamellae, taken to be a function of lamella orientation. Eight parameters are listed for describing four different types of crystallite orientation within the lamellae. Three parameters are believed sufficient, in principle, to describe spherulite deformation. These parameters are related to: (1) the transition in crystal orientation from (a) *b*-axis, oriented parallel to lamella axis, to (b) rotation of the crystallite around its own *a*-axis, and to (c) unfolding of folded chain crystals, (2) the fraction of crystallites that have random orientation within the lamellae, and (3) the fraction of crystallites that have orientation from unfolding rather than from rotation about the *a*-axis. With regard to nylon 6 spherulitic deformation, Matsuo *et al.* [143] list eleven parameters; the five most important describe the reorientation of nylon 6 crystallites within the orienting lamellae in such fashion that their molecular *b*-axes orient in the stretching direction. Problems arose on calculating molecular polarizability of the surrounding medium in which the crystallite scattering elements are embedded, because of a considerable contribution from hydrogen bonds.

Haas and MacRae studied biaxial deformation of high-density polyethylene [145] and poly-1-butene [146] films and observed that fracture initiated at the spherulite centres whereas deformation was localized at both the spherulite centres and at the boundary intersections. They surmised that the individual lamellae in the spherulites were under radial tension with this mode of deformation, and, because of "branching" of lamellae, there are fewer lamellae available to carry the force approaching the spherulite centre, thereby resulting in a stress concentration at the nucleus. This phenomenon was observed in both polyethylene and poly-1-butene, although the latter was observed to deform affinely, while the former deformed locally, i.e. "necked". Such behaviour was attributed to possibly more intercrystalline links in poly-l-butene. When spherulitic films were crystallized with large amounts of rejected material or large voids along the (spherulitic) boundaries, cracks formed and propagated from these areas.

Subsequently, Olf and Peterlin [147] investigated the crazing of smectic and monoclinic polypropylene at liquid-nitrogen temperatures. They noted that the crazes induced in the smectic polypropylene were similar to those found in glassy amorphous polymers and concluded that the small spherulites had no influence on craze propagation, either due to their small size or to highly disordered crystals. In monoclinic polypropylene, crazing occurred along spherulite diameters roughly transverse in the stress direction. The crazes run between stacked lamellae, possibly because of a separation along the amorphous surface layers between successive lamellae [147]. The presence of a condensed gas plasticized the amorphous material, reducing the work needed for formation of new surface and facilitating craze nucleation and propagation.

3.4. Amorphous orientation

Another question concerning the deformation of semi-crystalline polymers is whether or not the amorphous regions become oriented. From the fringed micelle theory, it has been concluded that these regions would have to be aligned in the draw direction much as the crystals [88] but when chain-folding is considered, the problem becomes more complex, and above the glass transition temperature T_g, segmental motion could dissipate amorphous orientation. Still, it is hard to imagine complete amorphous disorientation, when crystallites are known to be highly oriented; on the other hand, total amorphous orientation is also hard to envision, when one considers chain-folds and unstretched tie-molecules as part of the amorphous contribution. Amorphous orientation has been found in drawn polyethylene by polarized infrared spectroscopy [148]. This orientation is said to increase the content of the lower energy *trans* conformations and facilitate a better chain-packing which increases the density [149]. Chappel [150] studied crystalline and amorphous orientation in nylon 66 fibres by means of dichroism and birefringence. He found that the orientation of crystalline regions exceeded that of the amorphous regions at all stages of drawing and most noticeably in the early stages. Stein and Norris [151] also found this to be true with polyethylene, and found that at high extension ratios amorphous orientation

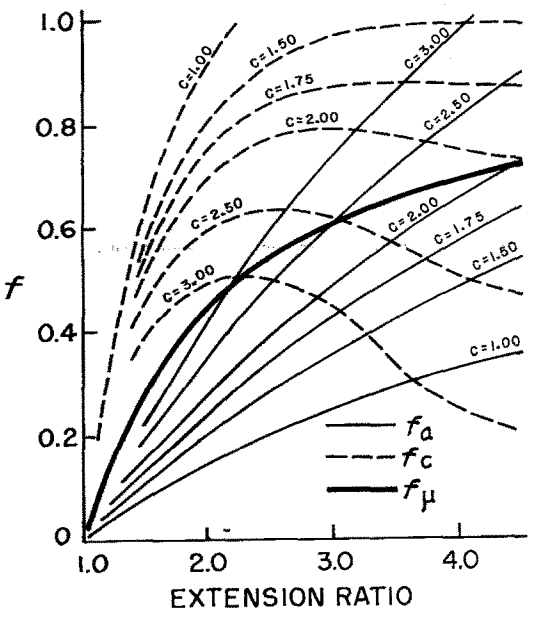

Figure 9 Graphs of f_a, f_c, and f_μ versus extension ratio for different values of c. Symbols explained in text. (after Chappel [150]).

reached a limit. Chappel, on the other hand, found that the amorphous orientation in nylon 66 showed no sign of reaching a limit up to the maximum extension realizable, although the rate of increase with extension ratio did decrease slightly at the highest extensions [150]. This is shown in Fig. 9 where f_a and f_c are the orientation functions of the amorphous and crystalline regions and f_μ is the birefringence orientation factor; C is a constant including the dichroic ratio of a perfectly oriented filament.

Samuels [139] used birefringence and sonic modulus techniques to measure amorphous orientation of stretched isotactic polypropylene films. They found that the amorphous orientation function, f_{am}, increased up to the highest extension investigated of 800%. He also found that tenacity and modulus correlate well with the amorphous orientation. Data indicated that shrinkage, as relaxation of noncrystalline chains, occurred via a common mechanism for all semicrystalline polymers below the melting point.

Nylon 610 has been cold-extruded by Yemni and Boyd [152]. They measured dielectric relaxation of both oriented and unoriented specimens in order to determine amorphous orientation. They found, with oriented specimens, that the intensity of the parallel dielectric loss factor was nearly zero, but the perpendicular loss was also reduced compared to the unoriented nylon 610. The other relaxation parameters (loss width and location) were nearly unaffected. They surmize that since the amide dipole is nearly perpendicular to the chain axis, orientation of the amorphous domains would result in very low loss in the parallel direction, while the perpendicular loss should be greater than in the unoriented case. However, because the dipole directions alternate in the extended conformation, a considerable degree of chain-alignment parallel to the draw direction would cause the observed decrease in the perpendicular loss [152]. These results are attributed to considerable amorphous phase orientation. Birefringence studies on isostatic polypropylene [153] and polyethylene [134] have also shown orientation of the amorphous component.

Peterlin [108] has shown that annealing of highly drawn crystalline polymers heals crystal defects but reduces drastically the number of tie-molecules. As a consequence of the loss of taut tie-molecules, the amorphous orientation disappears to the same extent as does the microfibrillar structure.

In summary, from the aforementioned studies it appears that the amorphous regions of drawn semicrystalline polymers are at least partially oriented. However, the extent of amorphous orientation and its relation to the extent of draw varies among polymers as may be expected. Likely variables include composition, molecular weight, temperature, original morphology preparation conditions, and extent of draw and annealing.

3.5. Annealing

Post-drawing annealing is a prime variable. On annealing cold-drawn polyethylene at or above 118° C, rapid relaxation occurs, manifesting itself in a long period increase for the crystal lamellae, an increase in density (crystallinity), and an increase in the heat content of the amorphous component to the value of completely relaxed chains [89]. Peterlin asserts this is all due to an entropic restoring force acting on strained uncrystallized tie-molecules which are given mobility by the high temperature. In the case of long period growth, the driving force is said to be the reduction of surface energy which reduces the crystal surface-to-volume ratio [21, 154]. Relaxation of tie-molecules increases the intramolecular (changes from *trans* to *gauche* conformations) and intermolecular energy [89]. In summary, Peterlin sug-

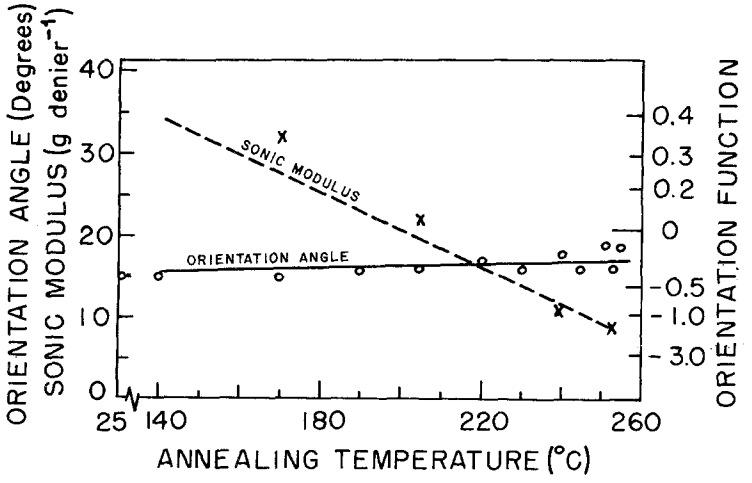

Figure 10 Change of orientation of nylon 66 with temperature (after Dismore and Statton [156]).

gests that annealing smoothes out the fold-surfaces, heals crystal defects, and relaxes the highly strained tie-molecules. This is consistent with the increase in small-angle scattering intensity [155] due to an increase in density difference between lamellae and the (amorphous) intermediate regions.

Dismore and Statton [156] investigated the effects of annealing on oriented nylon 66 fibres using X-ray diffraction, MNR, density measurements, and tensile testing. Their results show that on heating to 160 to 255° C under zero tension, some of the molecules change from elongated to folded conformation. They also noted, on heating below the melting point, an increase in percent crystallinity and a larger proportion of fluid-like segments. They attribute the latter to an increase in defect concentration with annealing. Sonic modulus also decreased with annealing temperature from 160 to 250° C, as shown in Fig. 10. The increased mobility may be attributed to disorientation of the amorphous phase. Annealing did not appreciably reduce crystal orientation but did lower the strength (Fig. 11) and elongation to break, likely due to fewer tie-molecules carrying the load [156]. Unmelted, albeit annealed, intermolecular bonds appeared to prevent overall crystal deorientation.

Another study of annealing effects of drawn nylon 66 was performed by Beresford and Beven [157]. They investigated the consequences of annealing by wide- and small-angle X-ray diffraction. Consistent with others [155, 156, 158], they noted increases in both long period and small-angle scattering intensity. As a result of their observations, a model for the structure of drawn polyamide fibres was proposed which consists of chain-folded molecules aggregated into ordered states which vary between the extremes of discrete lamellar regions with a few tie-molecules and regions in which the molecules are so irregularly folded and arranged that individual lamellae are no longer distinguishable [157], (see Fig. 12).

Mead and Porter [159] studied the effects of annealing on a highly-oriented linear polyethylene morphology containing ~15% extended chains [160]. They found that annealing between 126 and 132° C split the melting endotherm into two peaks at 132 and 139° C, the latter was the melting point of the unannealed (fibre) sample, while the former (132° C) was the melting temperature of the unoriented starting material. This and other results were consistent with the thermal instability associated with the anisotropy of the

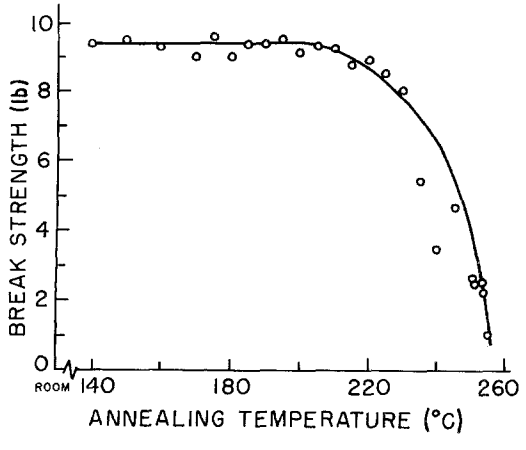

Figure 11 Change of breaking strength with temperature of three month old samples of nylon 66 (after Dismore and Statton [156]).

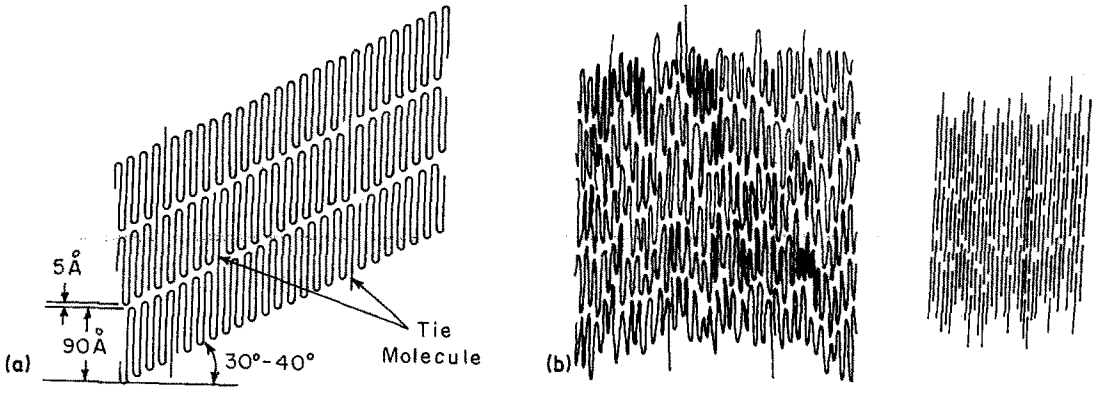

Figure 12 (a) Model comprising folded chains having well defined lamellar regions. (b) Arrangement of folded sheets which do not give low-angle reflections. (after Beresford and Bevan [157]).

surface free energies of their highly-oriented crystalline fibres of HDPE.

3.6. Mechanical properties

The effect of drawing on the dynamic mechanical properties of nylon 66 has been investigated by several authors [161–164]. Dumbleton and Murayama [104] found several interesting results. They noted that the tensile storage modulus (E') curves for samples parallel and perpendicular to the stretch direction (drawn 3 x) do not cross (with E' parallel always greater than E' perpendicular) in agreement with the work of Takayanagi *et al.* [165] on cold-drawn polypropylene and polyethylene (Fig. 13). The latter curves were found to cross when the (PE and PP) samples were annealed (Fig. 14). At a draw ratio of 4.5 x, Dumbleton and Murayama discovered that the nylon 66 curves do cross. They attribute this to annealing during drawing. These authors also noted other effects: (1) The crossing of the E' curves, for suitably treated samples, may be taken as evidence that the α transition* corresponds to the glass transition in nylon 66. (2) As the draw ratio increases, E' increases and the maximum in E'' (loss modulus) occurs at higher temperatures. The latter is usually indicative of increased crystallinity and/or a more closely packed morphology [162]. (3) There was no effect of annealing on the temperature of α up to the maximum temperature studied of 240° C. These authors [161] conclude that nylon 66 is probably a paracrystalline structure and that the α transition (T_g) may be a multiple transition.

Murayama and Silverman [162] studied the effects of molecular weight on the dynamic mechanical properties of nylon 66 film and fibre. They found that the α transition (glass transition) moved to higher temperatures (88 to 120° C) with increasing viscosity-average molecular weight ($\bar{M}_w$) from 45 000 to 120 000 for the film, and a shift from 110 to 123° C with an increase in $\bar{M}_w$ from 35 000 to 52 000 for the fibre. These authors concede that the α peak of high molecular weight nylon 66 may be affected by formation of additional interlamellar connections, as pointed out by Miyagi and Wunderlich [166].

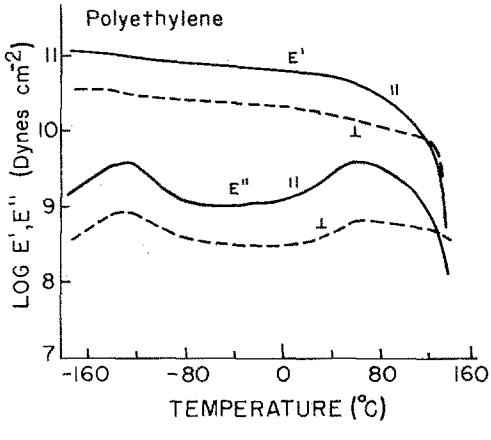

Figure 13 Temperature dependence of E' and E'' along and perpendicular to the drawing direction for the cold-drawn samples of linear polyethylene at 110 cycle sec^{-1}. (after Takayanagi *et al.* [165]).

*This α transition for nylon 66 is the glass transition, not to be confused with the (crystalline) α transition generally associated with semicrystalline polymers.

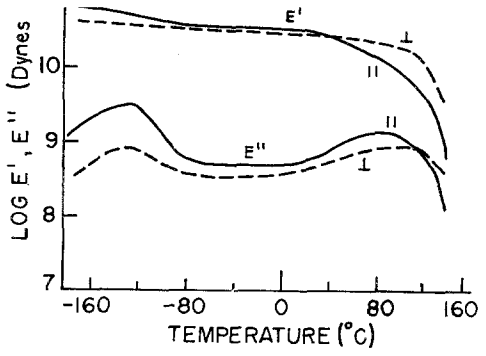

Figure 14 Temperature dependence of E' and E'' along and perpendicular to the drawing direction for the annealed samples of polyethylene at 110 cycle sec^{-1}. (after Takayanagi *et al.* [165]).

3.7 Polymorphism

Many cases of polymorphic transformations during polyethylene deformation have been reported [167–174]. Seto *et al.* [167] first cold drew then laterally compressed samples of high density polyethylene and noticed changes in texture of both the orthorhombic and monoclinic crystals formed. They attribute the textural changes to three possible deformations: (1) twinning and slip of crystal planes, (2) phase transformation (orthorhombic to monoclinic), and (3) slip at the grain boundaries (crystallite boundaries). Earlier investigations had revealed stress-induced transformations from an orthorhombic to a pseudohexagonal [168], triclinic [169, 170] or monoclinic [171] unit cell. Kiho *et al.* [171] reported that either twinning or a phase transformation occurs as a function of stretching. These authors also noted that the monoclinic X-ray reflections disappeared when deformed single crystals were allowed to relax [175]. They further showed that the monoclinic cell is unstable above 110° C [176]. In agreement, Seto *et al.* [167] found that the monoclinic form either reverted to the orthorhombic form, or twinned, or underwent both processes upon removal of the compressive stress. They attributed this to restoring forces caused by elastically-distorted amorphous regions between crystallites.

More recent results [173, 174] present an in-depth discussion of twinning and phase transformation modes in crystalline polyethylene and martensitic transformation to the monoclinic cell results from simple shear deformation of the orthorhombic cell. Young and Bowden [173] deformed oriented high-density polyethylene by shear perpendicular to the chain direction and examined the results by WAXS. They concluded that (1) the initial orientation relationship between the monoclinic and orthorhombic forms of polyethylene corresponds closely to the Tl_2 martensitic transformation mode of Bevis and Crellin [174], (2) the orientation of the monoclinic cell may change by slip during deformation or by twinning, on unloading (as did Seto *et al.* [167], (3) during a general deformation both [0 0 1] slip and the martensitic transformation should be activated, (4) (1 0 0) [0 1 0] transverse slip takes place when (1 0 0) is oriented at about 45° to the compression direction, and (5) (1 1 0) twinning is observed both during deformation and on unloading specimens. No evidence for (3 1 0) twinning was found.

Some studies have been made of the effect of drawing on polymorphic (crystal–crystal) transitions in nylon 6 [48, 158, 177]. Miyasaka and Makishima [177] treated nylon 6 multifilament yarns with aqueous iodine. In agreement with Bradbury [46], the new crystal structure was found by X-ray to be approximately the hexagonal γ-phase. The γ-phase is known to be stable to thermal (annealing) treatment [41]. When the treated sample was stressed in the chain direction $\geqslant 3.5 \times 10^3$ kg cm^2, a crystal reversion was found to occur (back) to the α-phase. This α-phase remains unchanged when heated for one minute at 100° C in water without tension.

In the γ-phase the chains are twisted about amide groups. When stretched, they assume the planar zigzag conformation characteristic of the α-phase. For hydrogen bonding to be complete in this new form (α), the adjacent chains must be antiparallel, as proposed by Arimoto [47], Bradbury [46], and Holmes *et al.* [178] (Fig. 15).

Sakaoku *et al.* [158] found that nylon 6 fibres drawn greater than 4 x and nylon 6 fibres annealed at 215° C, originally in the β-phase, were converted in large part to the α-phase. Such an effect had been noted previously [179, 180]. These α-phase crystals are shown to be more stable and increase their long period less on annealing [158].

In somewhat related work, changes in the hydrogen bonded structure of nylons above and

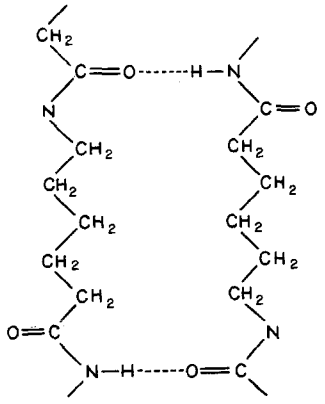

Figure 15 All hydrogen bonds made perfectly by inverting alternate chains. (after Holmes *et al.* [178]).

below T_g were investigated. Northolt [252], working with quenched nylon 11 film drawn 4 x, found biaxial orientation with samples drawn below the glass transition temperature (60° C) while uniaxial orientation prevailed when drawing took place above T_g. Identical behaviour was found with nylon 66, while only uniaxial orientation of crystallites was observed when nylon 12 was drawn at temperatures both below and above T_g (42° C). Northolt attributed the orientation behaviour to the nature of the hydrogen bonding in nylons 11, 12, and 66. Based on an idea by Gordon [253] that the glass transition in nylons is caused by disruption of hydrogen bonds in amorphous regions, Northolt postulates that for nylon 11 and nylon 66, the two dimensional (0 1 0) hydrogen bonded sheets produce biaxial orientation below T_g, while disruption of these sheets above T_g results in uniaxial crystallite orientation. In the case of nylon 12, a three-dimensional hydrogen bonded network, resulting from a hexagonal unit cell, and leading to a uniaxial orientation at all drawing temperatures, is said to exist [252].

4. Deformation processes

Three basic solid-state deformation processes have been used to achieve polymers of extreme modulus and tensile strength. These are cold drawing, cold extrusion and hydrostatic extrusion. The methods are interrelated with each having its distinct features.

4.1. Cold-drawing

Cold-drawing is a process that has been widely employed with both crystalline and amorphous polymers. It is characterized by load–elongation curves having three distinct regions, as shown in Fig. 16. The stress first rises, almost linearly, as the specimen is stretched. Next, the curve dips as a neck forms in the sample and consequently the stress falls at first, then is nearly constant and the neck propagates as stretching is continued. The length of necked-down (smaller diameter) region thus moves along the specimen until it is all drawn. At that stage, there is a marked increase in the stress on further extension, i.e., modulus increases, because the molecules aligned on necking, resist further elongation. Thus, during cold-drawing, there is a strain-hardening process that comes about as a result of the orientation of the molecules as part of the necking process. This orientation strain-hardening process increases the strength in the stretching direction many fold, and is responsible for the usefulness of commercial synthetic fibres which are commonly cold-drawn continuously during manufacture [184].

The "natural draw ratio" is the ratio of the length of a cold-drawn segment to the original undrawn length. It may also be defined as the smallest uniform draw ratio which can be given to a fibre or a film when it is oriented by cold-drawing rather than by uniform extension [181]. The natural draw ratio for a given polymer is

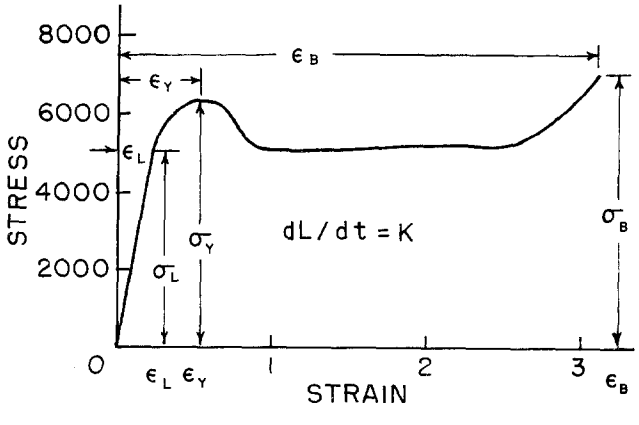

Figure 16 A schematic stress–strain curve. (after Nielsen [182]).

affected by experimental conditions [182] and polymer molecular weight [183]. For amorphous polymers, cold drawing occurs most readily just below the glass transition temperature, T_g. For semicrystalline polymers, cold-drawing may take place from below T_g up to near the melting point [181]. Other phenomena can occur at temperatures lower and higher than the cold-drawing range [181]. Such deformations, however, do not result in the same extent of molecular orientation as obtainable by cold-drawing.

The principles of cold-drawing have been discussed by many authors [185–191], not all of whom agree with each other. However, the basic facts seem to be that a non-uniformity (with regard to mechanical response) develops in the specimen under tensile stress, possibly due to a region of smaller cross-sectional area or because of stress concentrations [190]. The resultant local increase in stress causes an increase in strain, which results in a thinning at that point. Eventually the system becomes unstable, and a neck is formed. The edges of the neck deform rapidly, producing a local heating and temperature rise, and the neck thus propagates while the rest of the specimen resists deformation [191]. The local heating, i.e. strain-softening in the shoulders of the neck, leads to material in the neck zone becoming much stronger and stiffer in tension.

Under ideal conditions for a particular polymer, high draw can be achieved, resulting in polymers of high moduli and tensile strengths. Among investigators who have realized such properties are Ward [183, 192–195, 211], Clark [2], and Keller [196], each with coworkers. Andrews and Ward [192] tested a number of processing parameters in drawing tests on a high-density polyethylene. They found that the yield stress appeared to be a linearly increasing function with the logarithm of strain rate while the drawing stress, after initially increasing at about the same rate as the yield stress, subsequently dropped off (Fig. 17). The natural draw ratio was found to be independent of strain rate up to about 5×10^{-2} sec^{-1}, above which it increased rapidly. The authors attribute the increase to strain softening at the shoulders of the neck, due to adiabatic heating at higher strain rates. The natural draw ratio was only slightly affected by temperature, decreasing slightly up to 100° C possibly due to annealing, then increasing as the drawing temperature was raised further. The increase was attributed to melting of low molecular weight material, leading to nonhomogeneous deformation on drawing. The maximum natural draw ratio achieved in these studies was 15. Other conclusions of this work [192], were (1) the natural draw ratio decreases with increasing weight-average molecular weight, and (2) Young's modulus increase monotonically with increasing natural draw ratio. Higher molecular weights presumably provide a greater number of interlamellar-tie molecules [213] which impede crystal orientation, causing a lower natural draw ratio and subsequent lower Young's modulus; that is, a greater concentration of interlamellar ties supposedly increases the rate of strain hardening. Vincent [190] has shown that there is a lower limit of molecular weight for cold-drawing, below which there is insufficient strain hardening to stabilize the neck.

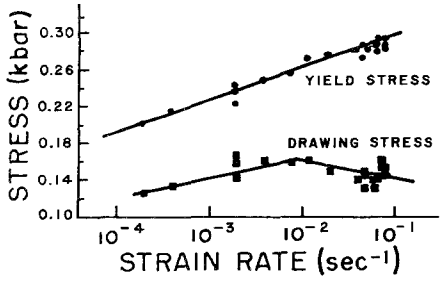

Figure 17 The effect of strain rate on the yield stress and drawing stress. (after Andrews and Ward [192]).

Capaccio and Ward [183, 193–195] have reported on the attainment of draw ratios to approximately 40. One study [194] concentrated on the preparation of the initial morphology. It was concluded that the sample component of highest molecular weight determines the highest tensile modulus attainable. The authors also proposed that molecular weight-dependent parameters such as the extent of crystal nucleation, crystal growth, and segregation of low molecular weight material, influence the initial morphology and thus the subsequent drawing. The maximum tensile modulus attained in this study was 69 GPa, measured at a draw ratio of 30 [194].

A further result by these authors [183] supported their contention that variations in the high molecular weight tail in the molecular weight distributions for their test polyethylene was likely the dominant feature influencing draw. Here they reported a strength greater than 0.35 GPa and a low elongation to break, ~3%. Capaccio and Ward [195] found that the yield stress increases with the crystallinity of the starting high density poly-

ethylene at constant molecular weight. The yield stress also increases with molecular weight at constant temperature. They concluded that the longer molecules in the distribution can form a network superstructure due to physical cross-linking by molecular entanglements. They further state that high values of $\bar{M}_w$, and crystallization under conditions where there are many tie-molecules linking the crystalline domains, both affect the morphology in a similar manner and reduce the maximum attainable draw ratio (and subsequently the modulus) achieved under standard conditions of draw.

Clark and Scott [2] carried out cold-drawing experiments on polyoxymethylene up to a draw ratio of about 20. This was achieved by a two-step drawing process at elevated temperature. During the first stage, the polymer was drawn to its natural draw ratio of about 7. The second step involved subsequent drawing at a very slow rate to a draw ratio of about 20. The mechanical properties of the resultant material (tensile strength: 1.7 GPa, Young's modulus: 35 GPa) exceeded prior values for this polymer [2]. A model was proposed where the chain-folds act as isolated units, existing as defects in a continuous crystal matrix as shown in Fig. 18. Thus, the authors claim, while chain-folds may be regions of weakness, the weakness is not magnified by aggregation of these defects into a chain-folded surface to create a mechanism for stress crack propagation, reducing the ability to draw.

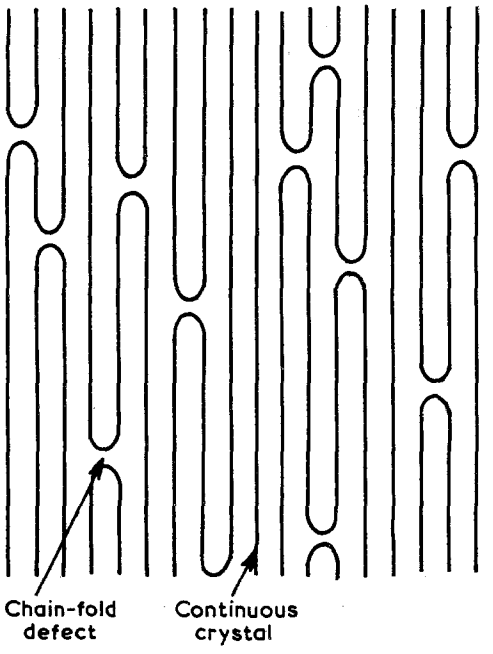

Figure 18 Model of continuous crystal matrix with chain-fold defects. (after Clark and Scott [2]).

Barham and Keller [196] have drawn single crystal mats and spherulitic sheets of polyethylene. They concluded that a component of low molecular weight was necessary to achieve high draw ratios. High temperatures ($\geqslant 75^\circ$ C) of drawing and slow crystallization of the starting material were also seen as important requirements for attaining high draw. They further noted that pulling out of chain-folds in the drawn fibre cannot be complete because they found a contraction on heating close to the melting point [197], a phenomenon not observed in crystals actually formed from pre-extended chains by primary crystallization. They believe that the folds remaining in drawn fibres are responsible for locked-in stresses.

Other workers have obtained high strength polypropylene [198, 199] fibres by cold-drawing, and also polyoxymethylene, nylon 6 and poly (vinyl alcohol) [200].

4.2. Cold extrusion

Cold extrusion is a relatively recent development [1, 201–206]. The polymer process is analogous to that used in obtaining profiles from ductile metals [207]. The process consists of forcing a solid plug of polymer, commonly by high pressure, through a die having a tapered entrance region [208]. This is shown schematically in Fig. 19. The resulting reduction ratio in cross-sectional area (plug to extrudate) is variously known as extrusion ratio, deformation, ratio, draw ratio, or degree of processing. The process imparts an elongational

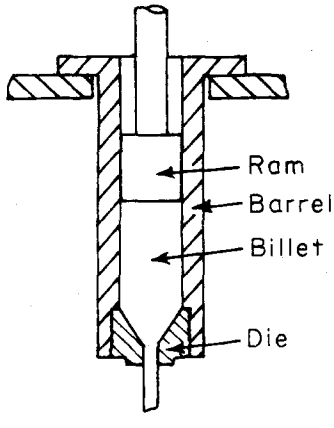

Figure 19 Schematic of solid state ram extrusion apparatus. (after Buckley and Long [212]).

deformation to polymer molecules [214] which results in remarkable physical and tensile properties [92, 204, 205, 209–212]. This solid-state extrusion process has been applied to high density polyethylene [1, 201–206, 208, 212, 222], low density polyethylene [212], polypropylene [1, 212, 215, 222], nylon 66 [206, 212], nylon 6 [213, 215, 222], and also poly(phenyleneoxide), polyoxymethylene, polytetrafluoroethylene, and poly(vinyl chloride) [212]. Recently, nylons 11 and 12 have also been solid-state extruded, in this laboratory.

The success of this process depends on the deformation taking place under conditions where polymer crystals are readily deformed. This may well correspond to conditions above the so-called α transition temperature of the particular polymer. This transition defines a lower temperature for the region (the crystalline melting point is the upper boundary) wherein crystals may be plastically deformed without being fractured by rupture of covalent bonds. The transition and thus the deformation range probably change with pressure. It is important to note, however, that as the melting point is approached, the polymer chains will deform ever more viscously with ever less morphological change, even though the sample more readily changes shape. Clark and Scott suggest that the α transition temperature may commonly be about 30° below the melting point [2]. Cold extrusion experiments conducted below this temperature must involve extremely long times for molecular rearrangement and thus very slow extrusion rates. Raising the pressure to increase the extrusion rate may only result in fractured extrudate.

Nielsen [182] investigated polyethylene and found that in unbranched, slowly cooled and annealed material, the α transition temperature may be over 100° C, whereas if the polymer is branched, or if it is a copolymer, or if it is quenched from the melt, the α transition is lower. As the degree of crystallinity is decreased, the magnitude of the transition also decreases. According to Nielsen [182], the α transition may be correlated with crystallite size and the length of polyethylene sequences in a crystallite. He thus proposed that the transition may be related to the chain-fold lengths and occurs at a temperature where the folded chains can "recrystallize" in a time comparable to the time required to make the dynamic test or deformation.

Below the α transition, the crystallites are less able to deform plastically as they act more like chemical crosslinks. When deformed over a few percent, the covalent bonds, already stretched, lead to rupture, and the necessary pulling out of folded chain crystals into extended chain crystals is thus restricted. So, for attainment of high draw, an optimum temperature of drawing (and pressure for extrusion) will likely be found between the α transition temperature and the polymer melting point. Takayanagi *et al.* [1] found that the optimum temperature for the cold extrusion of polypropylene was 110° C, which is just the proposed α transition temperature.

Many investigators are studying problems associated with cold extrusion as will be discussed. A problem encountered in cold extrusion is the appearance of cracks or crazes that occur usually at higher ($\sim$30) extrusion ratios [1, 208, 217]. Work in this laboratory with high-density polyethylene has shown that, as extrusion temperature is reduced, the fractures occur at lower extrusion ratios, indicating that the polymer crystals are increasingly unable to plastically deform at the lower (extrusion) temperatures. Although the extrusion rate was slower at the lower temperatures, it nonethless may have been faster than the crystals could accommodate to plastically deform. These defects, which apparently are small fractures oriented at various angles to the extrusion direction, result in oriented extrudates but with markedly reduced tensile properties. At high draw, the frequency of fracture is increased, and the extrudate eventually fails under its own weight.

Cold extrusion involves the deformation of *semicrystalline* polymer. Corresponding deformation analyses for polymer *melts* [218–221] have nonetheless been applied in an effort to understand solid state deformation phenomena.

The origin of extrudate fracture has been investigated with respect to polymer melts flowing through conical, converging dies [218–220]. It has been concluded that fracture originates at a point where fluid elements are subjected primary to extensional deformation, in the capillary inlet. Shaw [220] has shown that lubrication of the conical entrances forces the melt to converge at a sharp angle of the die itself, rather than establishing a more gradual convergence dictated by a balance of shear and extensional forces in the entry region [221]. The lubricant was silicone vacuum grease. He proposed that lubricant can reduce shear

stresses and favour extensional flow, thus generating high tensile stresses which result in extrudate fracture. Shaw concludes that die design for minimum pressure drop is inconsistent with production of unflawed extrudates because such a design invariably increases axial extension rates. Furthermore, he states that minimizing shear deformation in die design may cause higher tensile stresses for many shear sensitive fluids.

Benbow and Lamb [223] investigated melt fracture processes using both silicone gum and polyethylene extruded through dies of different materials. They measured the critical shear stress at which the onset of melt fracture began. Their results indicate that the critical shear stress for branched polyethylene through brass dies is higher than that for silver steel dies and shows a slight temperature dependence, whereas critical stress is independent of temperature in the silver steel dies. Furthermore, the flow curves show a break in the case of the brass dies whereas no break is seen with extrusion through the silver steel dies. Other conclusions drawn from this work [223] are: (1) melt instability originates at the die wall near the entry to the die, (2) when the melt flow is unstable, slipping occurs along the die wall, (3) flow birefringence experiments suggest that the stress changes in a manner consistent with a stick-slip motion, and (4) interpretation of the onset of melt instability as being due to a breakdown of adhesion between the polymer and the die well is supported by the known dependence of the critical shear stress on molecular properties and external conditions.

Predecki and Statton [206] point out that the use of a lubricant in cold extrusion reduced the extrusion pressures, consistent with Shaw's [220] results, but that the efficiency of the molecular orientation was reduced. It was concluded that a combination of extensional and shear deformation gives the most effective orientation and chain extension.

In this laboratory, we have found that the use of lubricants when cold-extruding polyethylene can allow attainment of higher extrusion ratios. With lubricant, extrudate clarity may be diminished, due to lubricant coated on the extrudate surface, but the physical and mechanical properties have not been significantly reduced.

The effect of die entrance angle on extrusion pressure has been investigated by several workers [213, 215, 224]. Increasing the die entrance angle generally results in an increase in extrusion pressure. Imada and Takayanagi [224] explain this through a slip line analysis following the ideas of Hill [225]. They calculated the slip lines for extrusion through a slit die and showed that, by integrating the force along the wall, the extrusion pressure can be estimated on the basis of the slip planes generated. The calculated result is an increase in extrusion pressure with increasing entrance angle as generally found experimentally. Takayanagi *et al.* [215] suggest that this pressure increase with entrance angle is attributable to the change of stress, and consequently velocity distribution, especially around the capillary inlet. Predecki and Statton [206] noted that a small ($<10^{\circ}$) die angle was necessary to produce solid-state extrudates free of defects.

Smith *et al.* [226] point out that cold extrusion, like hydrostatic extrusion, is limited by the pressure buildup at high extrusion ratios. They note that this is due to the pressure dependence of the yield behaviour of polymers, which implies that higher yield stresses are required for deformation where there is any substantial hydrostatic component of stress. This latter fact was noted by Pae *et al.* [227] in an earlier work. This is consistent with the results of Buckley and Long [212] who found that a material of relatively high modulus, like nylon, requires a greater pressure for extrusion than a material of lower modulus, like polyethylene.

Extrusion pressures employed in the cold extrusion process range to several thousand atmospheres, depending on choices such as extrusion ratio and temperature, polymer, and use of lubricant. Nakamura *et al.* [1] found that the molecular weight dependence of extrusion pressure for polypropylene was small compared with the case of melt viscosity. They propose that this indicates that the local molecular interaction is a predominant factor in solid state extrusion.

Increasing extrusion temperature was found to increase the long period of cold-extruded polyethylene [205, 222] as shown in Fig. 20. This can be attributed to an annealing effect wherein the extruded folded chain crystals grow in long period and the extruded extended chain crystals revert back to longer folded chain crystals [159]. It could also be a consequence of the original crystals being prepared at a higher temperature before extrusion. Imada and Takayanagi [224] also noted that polyethylene obtained at relatively low ex-

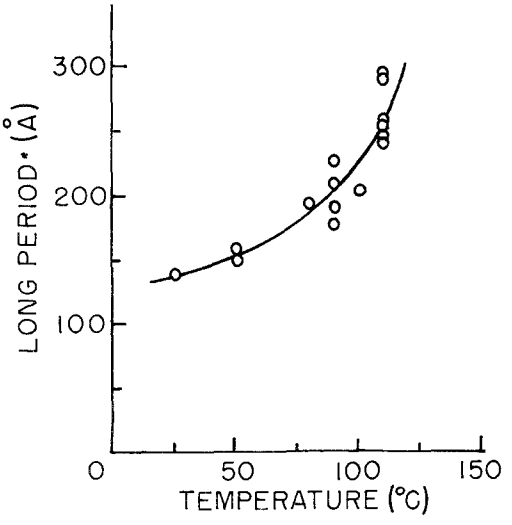

Figure 20 Long period of extrudates versus extrusion temperature. Points represent draw ratios from 4 to 25. (after Maruyama *et al.* [222]).

trusion temperatures (~80° C) showed elastic after-effects, such as shrinkage at elevated temperatures. However, that extruded at high temperatures (100 to 120° C) remained dimensionally stable, even at temperatures as high as 120° C. The two temperature ranges are respectively below and above accepted values for T_α. This implies that either (1) the extrudates obtained at the higher temperatures were substantially annealed in the extrusion process, or (2) amorphous orientation only occurs at low temperatures (below T_α), or (3) stable long periods were produced (at the higher temperatures) rather than shorter ones which were annealed. Another effect of increasing extrusion temperature may be a lower coefficient of friction at the polymer die interfaces resulting in lower extrusion pressure [222]. Further studies in this laboratory on the effects of extrusion temperature and ratio on cold-extruded polyethylene will be published [228].

Kolbeck and Uhlmann [229] extruded high density polyethylene, polypropylene, and poly (vinylidene fluoride), using a silicone or fluorocarbon lubricant on their dies. They observed what they believe to be necking of the deformed polymer within the conical entrance region of the die. (This could also result from relaxation of the compressed polymer upon the release of pressure prior to removal of the die). Deformational heating was minimal so melting and recrystallization during extrusion were presumed not to occur. During the initial stages of deformation, the predominant flow appeared to be elongational, whereas shear flow was indicated during later stages of extrusion. The authors observed that at large die angles (~40° included) the flow was dominated by shear rather than elongational flow. Kolbeck and Uhlmann conclude from their studies that both elongational and shear deformation are important in high stress extrusion, and that there are many similarities to extrusion in both the molten and crystalline state, leading them to believe that the amorphous component exerts a major influence on the extrusion of even highly crystalline polymers.

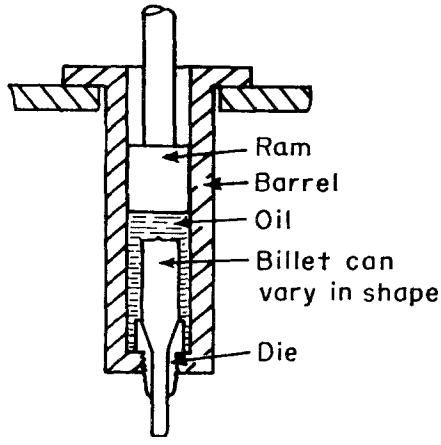

Figure 21 Schematic of solid state hydrostatic extrusion apparatus. (after Buckley and Long [212]).

4.3. Hydrostatic extrusion

Hydrostatic extrusion is similar to cold extrusion in that a ram or plunger is used to apply the extrusion pressure. In hydrostatic extrusion, pressure is transmitted through a fluid which surrounds the polymer plug, see Fig. 21. Frictional forces between the plug and container wall plus die are reduced by the presence of the pressurized lubricant. For these reasons, the pressure required for hydrostatic extrusion is lower, and the deformation approximates more closely a convergent flow [230]. This process is discussed by Williams [231], and by Yoon *et al.* [232], Fuchs [233], and by Alexander [234].

Hydrostatic extrusion has been predominantly applied to polyethylene [230, 235–238], although Buckley and Long [212] examined also polypropylene, nylon 66, polyoxymethylene, poly(vinyl chloride), poly(phenylene oxide) and polytetrafluoroethylene. Williams [231] hydrostatically extruded polypropylene, and Bhakja and Pae [239], a polyamide.

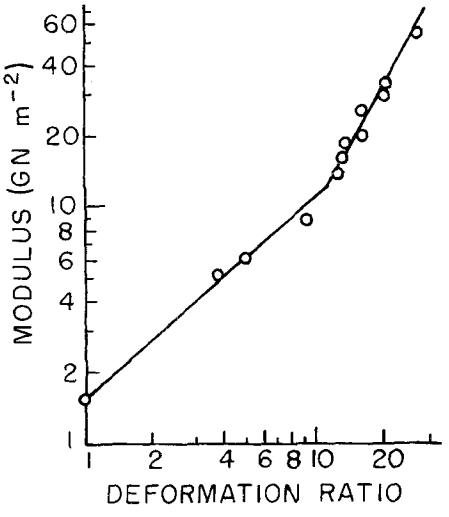

Figure 22 Effect of deformation ratio on the modulus of the extrudate (after Gibson *et al.* [230]).

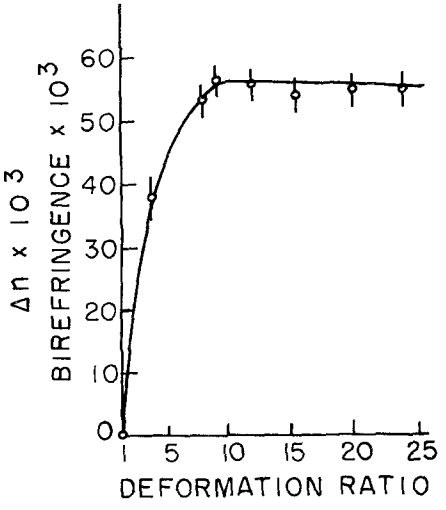

Figure 23 Variation of birefringence with deformation ratio (after Gibson *et al.* [230]).

Gibson *et al.* [230] investigated the hydrostatic extrusion of high density polyethylene using castor oil as the pressure transmitting fluid and silicone vacuum grease as a die lubricant. An extrusion ratio up to about 20 was achieved. Above an extrusion ratio of ~10, they noted a marked increase in modulus as shown in Fig. 22. This was also the point where the extrudate became transparent and the birefringence began to level off after initially increasing rapidly with extrusion ratio (Fig. 23). The authors propose that the morphology transformation to the fibre structure is essentially complete when an extrusion ratio of 10 has been reached. They believe that further deformation takes place by deformation of the fibre structure itself [107]. This is consistent with the common belief that high-density polyethylene has a natural draw ratio of ~11.

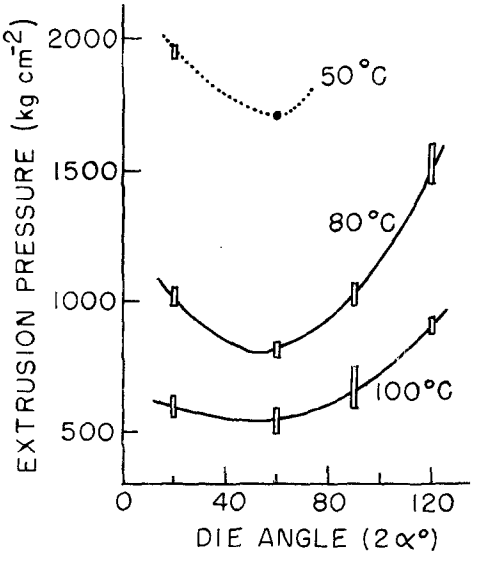

Figure 24 Extrusion pressure versus die angle. Extrusion ratio: 6.4 Plunger velocity: 5 mm min^{-1} (X): stick-slip. (after Nakayama and Kanetsuna [236]).

Davis [235] hydrostatically extruded high density polyethylene, using *n*-pentane, kerosene, oil, and water as extrusion fluids. He found that coating the die with PTFE reduced a severe stick-slip problem. The billet apparently stuck to the die until sufficient excess pressure built up, then it would extrude suddenly and completely at a high rate. Extruding into a fluid-filled reservoir also reduced this problem. Davis found that practical extrusion ratios are limited by shear failure of the extrudate as it exits the die rather than by excessive extrusion pressure, as is the case for metals. He also notes that solid state extrusion may prove useful for processing polymers unamenable to traditional processing techniques. This latter idea has been borne out in this laboratory with some high-melting (>300° C) aromatic polymers.

Nakayama and Kantesuna published three studies on hydrostatic extrusion of high density polyethylene [236–238]. They studied the influence of die angle, extrusion temperature and the extrusion ratio on the extrusion pressure and the appearance of the extrudate [236]. The included entrance angles used were 20°, 60°, 90° and 120° (Fig. 24). They classified extrusion pressure–displacement curves into three groups:

(1) Highly oriented extrudates having a smooth surface obtained by steady-state extrusion at higher temperature (100° C). (2) Extrusion at lower temperature with a larger entrance-angle die causing a stick-slip motion, which resulted in fluctuations in extrudate diameter. (3) High extrusion ratios where drastic stick-slip effects resulted in fractured extrudate. When extrusion was carried out through a small-angle die at constant pressure, a smooth transparent unflawed extrudate was obtained.

Another study by these authors involved an evaluation of the critical extrusion pressure and rate of extrusion using a simple die with a 20° included entrance angle [237]. A tensile testing machine, capable of sustaining a constant load on the billet, was used. Extrusions were carried out at 13 to 120° C and the minimum pressure required for extrusion was determined, see Fig. 25. This critical ressure decreased with increasing temperature, which also had a large influence on the relationship between the extrusion pressure and extrusion rate (Fig. 26).

The third study by Nakayama and Kantesuna investigated the effects of strain hardening and lubrication on extrusion pressure in hydrostatic extrusion of polyethylene [238]. Extrusion ratios (R'_E) of 3 to 9 were used. Critical extrusion pressure, P_0, i.e. minimum pressure required for extrusion, at different extrusion temperatures, T_E, was plotted against ln (R'_E). A rapid increase in the slope occurred at $\ln(R'_E) + (90 - T_E{}^\circ\text{C}) \sim 1.8$, which was associated with strain hardening. To investigate the strain hardening, the mean deformation resistance, σ_0, at each extrusion ratio, was estimated by using Pugh's equation. Several liquids

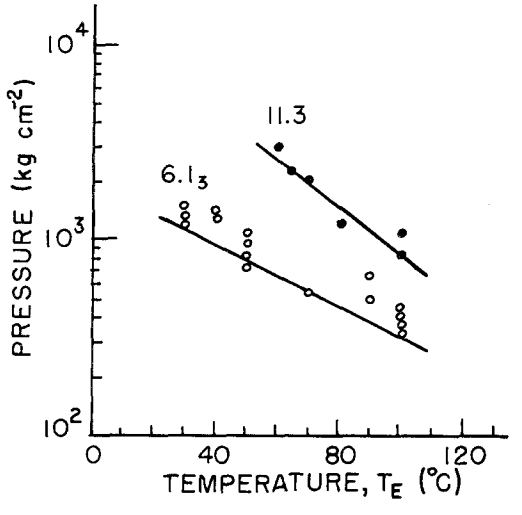

Figure 25 Extrusion pressure versus temperature. (○) extrusion ratio: 6.1, (●) extrusion ratio: 11.3. (after Nakayama and Kanetsuna [237]).

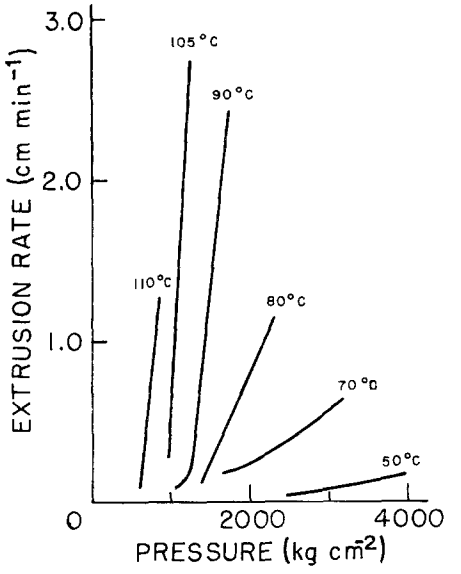

Figure 26 Extrusion rate versus pressure at extrusion temperatures shown. Extrusion ratio: 9.0 (after Nakayama and Kanetsuna [237]).

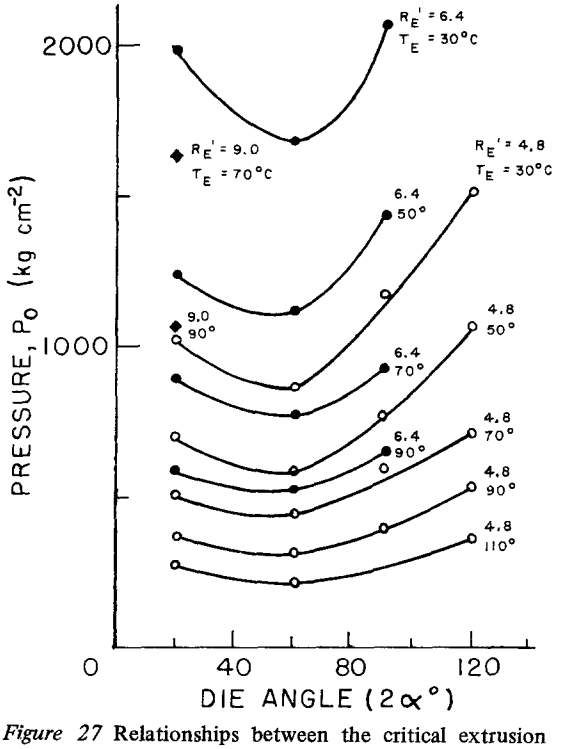

Figure 27 Relationships between the critical extrusion pressure P_0, and die angle 2α. R'_E: extrusion ratio (from 4.8 to 9). T_E: extrusion temperature (from 30 to 110° C). (after Nakayama and Kanetsuna [238]).

were used as the pressure medium to study lubrication effects. These included Molycote M-30, castor oil, glycerine, ethyl alcohol, glycerine–water, and water. When the critical extrusion pressure was plotted against included die entrance angle (2α), it was found that pressure first drops (at $\alpha = 20^\circ \rightarrow 60^\circ$) then rises (at $\alpha = 60^\circ \rightarrow 120^\circ$) with increasing entrance angle. This is shown in Figs. 24 and 27. This result contrasts with other investigators [213, 215, 224] who have found that extrusion pressure increases with increasing entrance-angle.

4.4. Other techniques

A process which has produced highly oriented and transparent strands of polyethylene and polypropylene has been developed by Collier *et al.* [240] using a commercial extruder with specially designed dies. The orientation is developed in the die entrance and is retained by crystallization in the die. Crystallization is reduced in the pre-die region by maintaining a temperature above the melting point of the flowing oriented melt. The procedure has the advantage of relatively low pressures and the possibility of being a continuous process.

Baranov *et al.* have utilized a process called "jet stretching" to deform and produce fibres of polyethylene [241], polypropylene [242], and nylon 6 [243]. The polymer is pumped through spinnerets at high speed and subsequently drawn at high rate at elevated temperatures. Small-angle polarized light scattering was used to characterize the structure as produced. The authors [243] postulate that the original (nylon 6) threads contain spherulites embedded in an amorphous glass-like matrix. They contend that stresses develop in this matrix, especially near the spherulite boundaries, and that these regions are subsequently destroyed, resulting in spherulite flattening which is reflected in the scattering patterns. At higher elongations, macrofibrils were observed in both optical micrographs and SALS patterns. Conclusions are that crystallization proceeds with the occurrence of molecular orientation which suppresses the growth of folded crystals in the direction of fibre formation.

Crystallization from a stressed melt was also carried out by Hashimoto and coworkers [244] using calendering equipment with linear polyethylenes of differing molecular weights. Hard elastic films, i.e. films which undergo a large elastic deformation on stretching along the machine direction, were produced from high molecular weight ($\bar{M}_w = 30$ to 35×10^4) polyethylene. The authors found that crystal lamellae were oriented with their normals parallel to the machine direction. *b*-axis orientation remained perpendicular to the machine direction whereas *c*- and *a*-axis orientation along the machine direction prevailed for the high and medium molecular weight polyethylenes, respectively. They noted that the proposal by Keller and Machin [245] that *c*- and *a*-axis orientation result, respectively, from crystallization under high and low shear stresses appeared to be applicable to their systems. The *c*-axis oriented films produced the hard elastic properties whereas the *a*-axis oriented films exhibited the usual yielding and necking. Hashimoto and coworkers conclude that the deformation of specimens along the machine direction involves lamellar bending and interlamellar slip, the former elastic in nature and the latter basically viscous and time-dependent. Both processes are thought to involve a plastic deformation of crystals.

Kwei *et al.* [246, 247] have developed a quench-rolling process for producing tough and transparent high-density polyethylene film. The preparation involves simultaneous high speed quenching ($10^{4\circ}$ C sec^{-1}) and shearing ($\sim 10^5$ sec^{-1}) of a polymer melt during crystallization. Two cold rotating metal rollers provide the shear and temperature gradient. Young's modulus, measured in the rolling direction is 4×10^{10} dynes cm^{-2} which is about 12 times higher than unoriented film and about twice the modulus of film drawn at room temperature 10×. The tensile strength of 1.04×10^9 dynes cm^{-2} is about seven times greater than unoriented film and slightly less than the 10× film.

Further studies on stress- (or strain-) induced crystallization can be found in the March, 1975, and 1976 special symposium issues of Polymer Engineering and Science, while a review by Biggs [248] discusses processes used for attainment of ultra-high moduli. A review on "hard elastic fibres", which are semicrystalline polymers crystallized under stress and retaining both high modulus and elastic recovery, has been published by Cannon *et al.* [249]. This paper elaborates on the morphology, mechanical properties, and physical mechanisms of these materials, which the authors term "springy polymers".

5. Summary and conclusions

Solid-state deformation has been used to achieve materials with ultra-high tensile moduli by taking advantage of the high strength of covalent bonds. This is accomplished by the pulling out of chain folds and subsequent extension of the molecular chains which run both through and between crystal lamellae. Three major processes detailed here are effective methods of aligning and extending chain-molecules in order to gain from them the strength and stiffness needed for many of today's and tomorrow's structural applications. The cold-drawing process has the advantage of adaptability to commercial equipment as now used to process polymer fibres. The cold extrusion technique brings another variable, pressure, into the picture, expanding the possibilities for more perfect uniaxial extension. The hydrostatic extrusion method, while in some cases messy, allows lower pressures and virtually eliminates frictional problems between polymer and processing equipment. While fracture at high extrusion ratios is a problem in cold extrusion, voiding at high draw ratios is likewise a problem with cold drawing, and interaction between the polymer and the pressure-transmitting fluid can lead to faulty results in the hydrostatic extrusion technique.

In some respects, the three types of solid-state deformation can be combined, as cold-drawing can be done under hydrostatic pressure [232, 250, 251] and the extrudates from both cold and hydrostatic extrusion can be drawn as they emerge from the die [231]. The latter technique is presently being investigated in this laboratory and preliminary results show increased rates of extrusion as well as the possibility of lower extrusion pressures.

Further research into the mechanisms of, and (optimum) conditions for, solid-state deformation will lead to more efficient processes and a yet closer approach to the high theoretical moduli of most semicrystalline thermoplastics.

6. Note added in proof

Farrell and Keller [255] have recently applied the technique of low frequency Raman spectroscopy to the characterization of solid-state extruded high density polyethylene. They found that upon deformation some molecular chains refold to a fold length appropriate to the processing temperature, while other chains *unfold* from lamellae. The unfolding leads to higher modulus and is more prevalent at the centre of the extrudate.

Pennings and co-workers have continued their series on the crystallization of polyamides under pressure [256–259]. One study [256] deals with the morphology and structure of pressure-crystallized nylon 6. Results indicated a brittle, extended chain morphology in which crystal perfection markedly increases with pressure. Despite large increases in crystallinity and a closer packing of chains, the concentration of free N–H groups is considerably enhanced, possibly due to the disturbance of antiparallel chains during chain extension [256]. No crystal structure modification was observed.

A companion study by these authors considered the effect of annealing nylon 6 under pressure [257]. It was found that greater crystal perfection could be obtained by annealing under pressure although there was evidence of thermal degradation in some of the samples. The highest melting point and heat of fusion measured was 269° C and 41.2 cal gm^{-1} respectively.

A third investigation combined pressure-induced crystallization and the annealing under pressure of nylon 11 [258]. Chain-extended crystals were formed from folded chain ones grown from the melt in the initial stage of crystallization under pressures exceeding 3 kbar. The heat of fusion and melting temperature were increased considerably by pressure-induced crystallization and by annealing under pressure.

Finally, nylon 12 was pressure-crystallized from the melt and subsequently annealed under pressure [259]. Both crystallization and annealing under pressure led to a partial transformation of the pseudo-hexagonal or monoclinic crystal structure to an alpha modification. Other results reported were multiple melting peak thermograms and a broadening of lamellar size distributions. Heat of fusion was doubled and melting point increased 30° C above the values for conventionally crystallized samples.

Burnay and Groves [260] deformed high density polyethylene to a compression ratio of 6.7 and examined the results by electron microscopy and X-ray diffraction. They noticed regions of highly misoriented lamellae which apparently do not affect X-ray patterns. These lamellae are thought to be remnants of spherulitic regions where no interlamellar or intermolecular shear forces were acting.

A clarification of apparently contradictory results regarding sample length changes with

lamellae spacing changes upon solid state deformation of polyethylene has been set forth by Pope and Keller [261]. They note that if both types of measurements are carried out at the temperature of deformation, all observed effects can be explained by known temperature-dependent structural processes. Nakayama and Kanetsuna have published part 6 of their series on the hydrostatic extrusion of solid polymers [262]. They observed considerable orientation and severe deformation of high density polyethylene crystallites at low deformation ratios, and rotation of crystallite blocks to the extrusion direction at higher ($\lambda > 4$) deformation ratios. Higher extrusion temperatures (70 to 110° C) resulted in higher Vickers hardness numbers and the extrudates with higher deformation ratios shrank the least when annealed at 100° C in water.

The effect of initial density (crystallinity) on the tensile properties of ultra-high molecular weight linear polyethylene was investigated by Trainor *et al.* [263]. The authors note, among other things, that the deformation mode changes from uniform extension to necking behaviour above a specific gravity of ~0.945, that yield stresses increases with increasing specific gravity, and that orientation hardening occurs with all materials studied, above about 200% extension. Strain at failure apparently decreases with increasing specific gravity (crystallinity).

A fibre composite model of highly oriented polyethylene has been recently proposed by Barham and Arridge [264] working at Keller's laboratory at Bristol. Crystalline fibrils are seen as deforming homogeneously during a secondary, taper-drawing process. The resulting increase in aspect ratio is believed to be responsible for the increase in tensile modulus owing to the increased efficiency of the fibrils as reinforcing elements. Further details and equations are presented in a quantitative description of what is phenomenologically observed.

Acknowledgements

The authors gratefully acknowledge financial support from the Engineering Division of the National Science Foundation (NSF), the Office of Naval Research (ONR), and the U.S. Army Materials and Mechanics Research Centre (Watertown). They also wish to express their gratitude to Drs E. Otocka and A. Peterlin for helpful suggestions during the preparation of this review.

References

1. K. NAKAMURA, K. IMADA, and M. TAKAYANAGI, *Inter. J. Polym. Mater.* **2** (1972) 71.
2. E. S. CLARK and L. S. SCOTT, *Polym. Eng. Sci.* **14** (1974) 682.
3. I. SAKURADA and K. KAJI, *J. Polymer Sci. C* **31** (1970) 57.
4. F. W. BILLMEYER, *J. Amer. Chem. Soc.* **75** (1953) 6118.
5. J. K. BEASLEY, *ibid* **75** (1953) 6123.
6. I. HARRIS, *J. Polymer Sci.* **8** (1952) 353.
7. C. W. BUNN, *Trans. Faraday Soc.* **35** (1939) 482.
8. R. L. MILLER, in "Crystalline Olefin Polymers", Part I, edited by R. A. V. Raff and K. W. Doak (Interscience, New York, 1965) Ch. 12.
9. E. R. WALTER and F. P. REDING, *J. Polymer Sci.* **21** (1956) 561.
10. A. RENFREW and P. MORGAN (editors) "Polythene", (Interscience, New York, 1960).
11. H. D. KEITH and F. J. PADDEN Jr., *J. Polymer Sci.* **39** (1959) 101.
12. *Idem, ibid* **39** (1959) 123.
13. A. KELLER, *J. Polymer Sci.* **39** (1959) 151.
14. F. P. PRICE, *ibid* **39** (1959) 139.
15. L. MANDELKERN, in "Growth and Perfection of Crystals", edited by R. H. Doremus, B. W. Roberts and D. Turnbull (John Wiley, New York, 1958) p. 467.
16. S. BUCKSER and L. H. TUNG, *J. Phys. Chem.* **63** (1958) 763.
17. L. MANDELKERN, M. NELLMAN, B. W. BROWN, D. E. ROBERTS and F. A. QUINN, *J. Res. Nat. Bur. Standards* **58** (1957) 137.
18. P. H. LINDENMEYER, *Polymer Eng. Sci.* **14** (1974) 456.
19. J. SCHULTZ, "Polymer Materials Science", (Prentice Hall, Englewood Cliffs, New Jersey, 1974).
20. F. J. BALTA-CALLEJA, D. C. BASSETT and A. KELLER, *Polymer* **4** (1963) 269.
21. I. C. SANCHEZ, J. P. COLSON and R. K. EBY, *J. Appl. Phys.* **44** (1973) 4332.
22. I. C. SANCHEZ, A. PETERLIN, R. K. EBY and F. L. McCRAKIN, *ibid* **45** (1973) 4216.
23. D. P. POPE and A. KELLER, *J. Polymer Sci. -Phys.* **14** (1976) 821.
24. M. YASUNIWA, C. NAKAFUKU and T. TAKEMURA, *Polymer J.* **4** (1973) 526.
25. M. KYOTANI and H. KANETSUNA, *J. Polymer Sci. -Phys.* **12** (1974) 2331.
26. Y. MAEDA and H. KANETSUNA, *ibid* **12** (1974) 255.
27. B. WUNDERLICH and T. ARAKAWA, *J. Polymer Sci. A–2* **2** (1964) 3697.
28. P. GEIL, F. R. ANDERSON, B. WUNDERLICH and T. ARAKAWA, *ibid* **3** (1964) 3707.
29. D. V. REES and D. C. BASSETT, *ibid* **9** (1971) 385.
30. J. M. LUPTON and J. W. REGESTER, *J. Appl. Polymer Sci.* **18** (1974) 2407.
31. G. E. ATTENBURROW and D. C. BASSETT, *J. Mater. Sci.* **12** (1977) 192.
32. D. C. BASSETT, *Polymer* **17** (1976) 460.
33. Y. KINOSHITA, *Makromol. Chem.* **33** (1959) 1.

34. G. CHAMPETIER and R. AELION, *Bull. Soc. Chim. France* (1948) 683.
35. R. HILL and E. E. WALKER, *J. Polymer Sci.* **3** (1948) 609.
36. D. D. COFFMAN, N. L. COX, E. L. MARTIN, W. E. MOCHEL and F. J. VANNATTA, *J. Polymer Sci.* **3** (1948) 85.
37. D. D. COFFMAN, G. J. BERCHET, W. R. PETERSON and E. W. SPANAGEL, *J. Polymer Sci.* **2** (1947) 306.
38. C. W. BUNN and E. V. GARNER, *Proc. Roy. Soc. (Lond.)* **A189** (1957) 39.
39. V. V. KORSHAK and T. M. FRUNZE, *Zhur. Obshchei Khim.* **26** (1956) 732.
40. D. S. TRIFAN and J. F. TERENZI, *J. Polymer Sci.* **28** (1958) 443.
41. A. MIYAKE, *ibid* **44** (1960) 223.
42. M. I. KOHAN, "Nylon Plastics", (John Wiley, New York, 1973).
43. D. R. HOLMES, C. W. BUNN and D. J. SMITH, *J. Polymer Sci.* **17** (1955) 159.
44. I. SANDEMAN and A. KELLER, *ibid* **19** (1956) 401.
45. R. HOSEMANN, *Polymer* **3** (1962) 349.
46. E. M. BRADBURY, L. BROWN, A. ELLIOTT and D. A. D. PARRY, *ibid* **6** (1965) 465.
47. H. ARIMOTO, *J. Polymer Sci. A–2* **2** (1964) 2283.
48. B. D'ALO, G. COPPOLA and B. PALLESI, *Polymer* **15** (1974) 130.
49. M. G. NORTHOLT, B. J. TAYLOR and J. J. VANAARTSEN, *J. Polymer Sci. A–2* **10** (1972) 191.
50. K. INOUE and S. HOSHINO, *J. Polymer Sci. Phys.* **2** (1973) 1077.
51. T. ISHIKAWA, A. SUGIHARA, T. HAMADA, S. NAGAI, N. YASUOKA and N. KASAI, *Kagaku* **9** (1973) 1744.
52. R. J. FREDERICKS, *J. Polymer Sci. A–2* **4** (1956) 899.
53. M. TSURUTA, H. ARIMOTO and M. ISHIBASHI, *Kobunshi Kagaku* **15** (1958) 619.
54. Y. KINOSHITA, *Makromol. Chem.* **33** (1959) 21.
55. D. C. VOGELSONG and E. M. PEARCE, *J. Polymer Sci.* **45** (1960) 546.
56. H. ARIMOTO, *Kobunshi Kagaku* **19** (1962) 212.
57. K. MIYASAKA and K. MAKISHIMA, *ibid* **23** (1966) 870.
58. R. BRILL, *J. Prakt. Chem.* (1942) 161.
59. P. W. ALLEN, *Research (London)* **5** (1952) 492.
60. H. M. HEUVEL, R. HUISMAN and K. C. J. B. Lind, *J. Polymer Sci. Phys.* **14** (1976) 921.
61. R. HUISMAN and H. M. HEUVEL, *ibid* **14** (1976) 941.
62. W. P. SLICHTER, *J. Polymer Sci.* **36** (1959) 259.
63. *Idem, ibid* **35** (1959) 77.
64. M. GENAS, *Angew. Chem.* **74** (1962) 535.
65. S. ONOGI, T. ASADA, Y. FUKUI and I. TACHINAKA, *Bull. Inst. Chem. Res. Kyoto Univ.* **52** *(2)* (1974) 368.
66. R. AELION, *Ann. Chim. (Paris)* **3** (1948) 5.
67. R. J. BARRIAULT and L. F. GRONHOLTZ, *J. Polymer Sci.* **18** (1955) 393.
68. H. W. STARKWEATHER Jr. and R. E. BROOKS, *J. Appl. Polymer Sci.* **1** (1959) 236.
69. H. W. STARKWEATHER Jr., G. E. MOORE, J. E. HANSEN, T. M. RODER and R. E. BROOKS, *J. Polymer Sci.* **21** (1956) 189.
70. H. W. STARKWEATHER Jr., *J. Appl. Polymer Sci.* **2** (1969) 129.
71. *Idem, J. Macromol. Sci. Phys.* **B-3** (1969) 727.
72. J. L. KOENIG and M. C. AGBOATWALLA, *ibid* **B-2** (1968) 391.
73. C. G. CANNON and P. H. HARRIS, *ibid* **B-3** (1969) 357.
74. F. KHOURY, *J. Polymer Sci.* **33** (1958) 389.
75. E. S. CLARK and C. A. GARBER, *Inter. J. Polym. Mat.* **1** (1971) 31.
76. A. KELLER and M. J. MACHIN, *J. Macromol. Sci. Phys.* **B-1** (1967) 41.
77. M. J. HILL and A. KELLER, *ibid* **B-3** (1969) 153.
78. J. MANN and L. ROLDAN-GONZALEZ, *J. Polymer Sci.* **60** (1962) 1.
79. J. H. MAGILL, *J. Polymer Sci. A–2* **4** (1966) 243.
80. C. R. LINDEGREN, *J. Polymer Sci.* **50** (1961) 181.
81. D. V. BADAMI and P. H. HARRIS, *ibid* **41** (1959) 540.
82. C. G. CANNON, F. P. CHAPPEL and J. I. TIDMARSH, *J. Text. Inst.* **54** (1963) T210.
83. J. V. McLAREN, *Polymer* **4** (1963) 175.
84. U.S. Patent 3 080 345, (March 5, 1963) to E. I. DuPont deNemours & Co.
85. A. D. McLAREN and J. W. ROWEN, *J. Polymer Sci.* **7** (1951) 289.
86. S. GOGOLEWSKI and A. J. PENNINGS, *Polymer* **14** (1973) 463.
87. *Idem, ibid* **16** (1975) 673.
88. T. ZYLINSKI, "Fibre Science" (S.P.F.C.C.C.I.S.T.E.I. Warsaw, 1964).
89. A. PETERLIN, *J. Polymer Sci. C* **15** (1966) 427.
90. *Idem, J. Polymer Sci. A–2* **9** (1971) 67.
91. N. W. WYCKOFF, *J. Polymer Sci.* **62** (1962) 83.
92. W. G. PERKINS, N. J. CAPIATI and R. S. PORTER, *Polymer Eng. Sci.* **16** (1976) 200.
93. W. URBANCZYK, *J. Polymer Sci.* **59** (1962) 215.
94. D. C. PREVORSEK and R. K. SHARMA, *Polymer Eng. Sci.* **14** (1974) 778.
95. D. C. PREVORSEK, P. J. HARGET, R. K. SHARMA and A. C. REIMSCHUESSEL, *J. Macromol. Sci. Phys.* **B-8** *(1–2)* (1973) 127.
96. A. C. REIMSCHUESSEL and D. C. PREVORSEK, *J. Polymer Sci. Phys.* **14** (1976) 485.
97. A. PETERLIN, *Polymer Eng. Sci.* **9** (1969) 172.
98. *Idem, J. Mater. Sci.* **6** (1971) 490.
99. *Idem, Text Res. J.* **42** (1972) 20.
100. *Idem, Ann. Rev. Mater. Sci.* **2** (1972) 349.
101. J. BECHT, K. L. DeVRIES and H. H. KAUSCH, *Eur. Polym. J.* **7** (1971) 105.
102. J. BECHT and H. FISCHER, *Kolloid-Z-Polym.* **240** (1970) 766.
103. H. D. KEITH and F. J. PADDEN, *J. Polymer Sci.* **41** (1959) 525.
104. D. C. PREVORSEK, *J. Polymer Sci. C* **32** (1971) 343.
105. A. PETERLIN, *J. Polymer Sci. A–2* **7** (1969) 1151.

106. G. MEINEL and A. PETERLIN, *ibid* 9 (1971) 67.
107. G. MEINEL, A. PETERLIN and K. SAKAOKU, in "Analytical Calorimetry", edited by R. S. Porter and J. F. Johnson (Plenum Press, New York, 1968).
108. A. PETERLIN, *J. Macromol. Sci. Phys.* 88 (1973) 83.
109. *Idem,* in "Copolymers, Polyblends and Composites", edited by N. A. J. Platzer, Adv. Chem. Ser. #142 (Amer. Chem. Soc., 1955) p. 1.
110. *Idem, Colloid Polym. Sci.* 253 (1975) 809.
111. *Idem, Polymer Eng. Sci.* 17 (1977) 183.
112. P. J. BARHAM, private communication.
113. M. TAKAYANAGI and T. KAJIYAMA, *J. Macromol. Sci. Phys.* B8 (1973) 1.
114. D. A. ZAUKELIES, *J. Appl. Phys.* 33 (1962) 2797.
115. R. HOSEMANN, *C.R.C. Crit. Rev. Macromol. Sci.* 1 (1972) 351.
116. *Idem, Acta Crystallogr.* 4 (1950) 520.
117. D. H. RENEKER, *J. Polymer Sci.* 59 (1962) 39.
118. W. PECHHOLD, *Kolloid Z.* 228 (1968) 1.
119. W. PECHHOLD and S. BLASENBREY, *ibid* 216 (1967) 235.
120. J. J. POINT, M. DOSIÈRE, M. GILLIOT and A. GOFFIN-GÉRIN, *J. Mater. Sci.* 6 (1971) 479.
121. D. M. GEZOVICH and P. H. GEIL, *ibid* 6 (1971) 531.
122. P. B. BOWDEN and R. J. YOUNG, *ibid* 9 (1974) 2034.
123. R. G. C. ARRIDGE, P. J. BARHAM and A. KELLER, *J. Polym. Sci. Phys.* 15 (1977) 389.
124. I. L. HAY and A. KELLER, *Kolloid-S-Polym.* 204 (1965) 43.
125. H. D. KEITH and F. J. PADDEN, *J. Polymer Sci.* 41 (1969) 525.
126. K. SASAGURI, S. HOSHINO and R. S. STEIN, *J. Appl. Phys.* 35 (1964) 47.
127. P. ERHARDT, K. SASAGURI and R. S. STEIN, *J. Polymer Sci. C* 5 (1964) 179.
128. R. S. STEIN, S. ONOGI, K. SASAGURI and D. A. KEEDY, *J. Appl. Phys.* 34 (1963) 80.
129. Y. F. YU and R. ULLMAN, *J. Polymer Sci.* 60 (1962) 55.
130. P. INGRAM and A. PETERLIN, *J. Polymer Sci.* B-2 (1964) 739.
131. J. L. COONEY, *J. Appl. Polymer Sci.* 8 (1964) 1889.
132. R. S. STEIN, *S.P.E. Trans.* 4 (1964) 1.
133. *Idem, Polymer Eng. Sci.* 9 (1969) 320.
134. *Idem, J. Polymer Sci. C* 1 (1966) 185.
135. *Idem, Polymer Eng. Sci.* 9 (1969) 320.
136. *Idem, Rheology* 5 (1972) 121.
137. *Idem. Acc. Chem. Res.* 5 (1972) 121.
138. R. YANG and R. S. STEIN, *J. Polymer Sci. A–2* 5 (1967) 939.
139. R. J. SAMUELS, "Structured Polymer Properties" (John Wiley, New York, 1974).
140. *Idem, J. Polymer Sci.* C13 (1966) 37.
141. *Idem, ibid* A3 (1965) 1741.
142. R. G. CRYSTAL and D. HANSEN, *ibid A–2* 6 (1968) 981.
143. M. MATSUO, H. HATTORI, S. NOMURA and H. KAWAI, *J. Polymer Sci. Phys.* 14 (1976) 223.
144. S. NOMURA, M. MATSUO and H. KAWAI, *ibid* 10 (1972) 2489.
145. T. W. HAASS and P. H. MACRAE, *S.P.E. J.* 24 (1968) 27.
146. *Idem, Polymer Eng. Sci.* 9 (1969) 423.
147. H. OLF and A. PETERLIN, *J. Coll. Sci.* 47 (1974) 628.
148. W. GLENZ and A. PETERLIN, *J. Macromol. Sci.* B-4 (1970) 473.
149. E. W. FISCHER, H. GODDAR and G. F. SCHMIDT, *Makromol. Chem.* 118 (1968) 144.
150. F. P. CHAPPEL, *Polymer* 1 (1960) 409.
151. R. S. STEIN and F. H. NORRIS, *J. Polymer Sci.* 21 (1965) 391.
152. T. YEMNI and R. H. BOYD, *J. Polymer Sci. Phys.* 14 (1976) 499.
153. R. J. SAMUELS, *J. Polymer Sci. C* 20 (1967) 253.
154. H. G. ZACHMANN, *Z. Naturforsch.* 19a (1964) 1397.
155. P. F. DISMORE and W. O. STATTON, *J. Polymer Sci.* B-2 (1964) 1116.
156. *Idem, ibid* C13 (1966) 133.
157. D. R. BERESFORD and H. BEVAN, *Polymer* 5 (5) (1963) 247.
158. K. SAKAOKU, N. MOROSOFF and A. PETERLIN, *J. Polymer Sci. Phys.* 11 (1973) 31.
159. W. T. MEAD and R. S. PORTER, *J. Appl. Phys.* 47 (1976) 4278.
160. N. E. WEEKS, Ph.D. Thesis, University of Massachusetts, 1974.
161. J. H. DUMBLETON and T. MURAYAMA, *Kolloid-Z-Polymer* 238 (1970) 410.
162. T. MURAYAMA and B. SILVERMAN, *J. Polymer Sci. Phys.* 11 (1973) 1873.
163. K. H. ILLERS, *Colloid Polym. Sci.* 253 (1975) 329.
164. T. MURAYAMA, J. H. DUMBLETON and M. L. WILLIAMS, *J. Makromol. Sci. Phys.* B-1 (1967) 1.
165. M. TAKAYANAGI, K. IMADA and T. KAJIYAMA, *J. Polymer Sci.* C-15 (1966) 263.
166. A. MIYAGI and B. WUNDERLICH, *Bull. Amer. Phys. Soc. (11)* 16 (1971) 410.
167. T. SETO, T. HARA and K. TANAKA, *Jap. J. Appl. Phys.* 7 (1968) 31.
168. W. P. SLICHTER, *J. Polymer Sci.* 21 (1966) 141.
169. P. W. TEARE and D. R. HOLMES, *ibid* 24 (1957) 496.
170. A. TURNER-JONES, *ibid* 62 (1962) 853.
171. H. KIHO, A. PETERLIN and P. H. GEIL, *J. Appl. Phys.* 35 (1964) 1599.
172. K. TANAKA, T. SETO and T. HARA, *J. Phys. Soc. Japan* 17 (1962) 873.
173. R. J. YOUNG and P. B. BOWDEN, *Phil. Mag.* 29 (1974) 1061.
174. M. BEVIS and E. B. CRELLIN, *Polymer* 12 (1971) 666.
175. H. KIHO, A. PETERLIN and P. H. GEIL, *J. Polymer Sci.* B-3 (1965) 157.
176. *Idem, ibid* B-3 (1965) 263.
177. K. MIYASAKA and K. MASKISHIMA, *ibid* A-1 5 (1967) 3017.
178. D. R. HOLMES, C. W. BUNN and D. J. SMITH, *J. Polymer Sci.* 17 (1955) 159.

179. A. ZIABICKI, *Colloid-Z.* **167** (1960) 132.
180. H. ARIMOTO, M. ISHIBASHI and M. HIRAI, *J. Polym. Sci. A-3,* 317 (1965).
181. P. I. VINCENT, "Fracture" in "Mechanical Properties of Polymers", edited by N. M. Bikales (John Wiley, New York, 1971) p. 105.
182. L. E. NIELSEN, "Mechanical Properties of Polymers" (Reinhold, New York, 1962) Ch. 5.
183. G. CAPACCIO and I. M. WARD, *Polymer Eng. Sci.* **15** (1975) 219.
184. E. I. DuPont deNemours and Co., U.S. Pat. 604 667.
185. J. MIKLOWITZ, *J. Colloid Sci.* **2** (1947) 193.
186. I. MARSHALL and A. B. THOMPSON, *Proc. Roy. Soc. A* **221** (1954) 541.
187. F. H. MÜLLER, *Rub. Chem. Tech.* **30** (1957) 1027.
188. K. JÄCKEL, *Kolloid-Z.* **137** (1954) 130.
189. J. S. LAZURKIN, *J. Polymer Sci.* **30** (1958) 585.
190. P. I. VINCENT, *Polymer* **1** (1960) 7.
191. Y. A. ANTSUPOV, U. P. VOLODIN and E. V. KUVSHINSKII, *Mekanika Polimerov* **4** (3) (1968) 509.
192. J. M. ANDREWS and I. M. WARD, *J. Mater. Sci.* **5** (1970) 411.
193. G. CAPACCIO and I. M. WARD, *Nature Phys. Sci.* **243** (1973) 143.
194. *Idem, Polymer* **15** (1974) 233.
195. *Idem, ibid* **16** (1975) 239.
196. P. J. BARHAM and A. KELLER, *J. Mater. Sci.* **11** (1976) 27.
197. *Idem, J. Polymer Sci.* **B-13** (1975) 197.
198. H. D. NOETHER and R. W. SINGLETON, U.S. Pat. 3 161 709 (1964).
199. W. C. SHEEHAN and T. B. COLE, *J. Appl. Polymer Sci.* 8 (1964) 2359.
200. S. N. ZHURKOV, B. Y. LEVIN and A. V. SAVITSKII, *Doklady Phys., Chem.* **186** (1969) 296.
201. J. H. SOUTHERN and R. S. PORTER, *J. Macromol. Sci. Phys.* **B-4** (1970) 541.
202. *Idem, J. Appl. Polymer Sci.* **14** (1970) 2305.
203. J. H. SOUTHERN, N. E. WEEKS and R. S. PORTER, *Makromol. Chem.* **162** (1972) 19.
204. R. S. PORTER, J. H. SOUTHERN and N. E. WEEKS, *Polymer Eng. Sci.* **15** (1975) 213.
205. K. IMADA, T. YAMAMOTO, K. SHIGAMATSU and M. TAKAYANAGI, *J. Mater. Sci.* **6** (1971) 537.
206. P. PREDECKI and W. O. STATTON, *J. Polymer Sci.* **B-10** (1972) 87.
207. CARROLL EDGAR, "Fundamentals of Manufacturing Processes and Materials", Addison–Wesley, Reading, Mass., 1965.
208. N. J. CAPIATI, S. KOJIMA, W. G. PERKINS and R. S. PORTER, *J. Mater. Sci.* **12** (1977) 334.
209. N. E. WEEKS and R. S. PORTER, *J. Polymer Sci. Phys.* **12** (1974) 635.
210. N. J. CAPIATI and R. S. PORTER, *ibid* **12** (1975) 1177.
211. D. L. M. CANSFIELD, G. CAPACCIO and I. M. WARD, *Polymer Eng. Sci.* **16** (1976) 721.
212. A. BUCKLEY and H. A. LONG, *Polymer Eng. Sci.* **9** (1969) 115.
213. K. IMADA, Y. KONDO, K. KANEKIYO and M. TAKAYANAGI, *Rep. Prog. Polym. Phys. Jap.* **14** (1971) 393.
214. C. D. DENSON, *Polymer Eng. Sci.* **13** (1973) 125.
215. S. MARUYAMA, K. IMADA and M. TAKAYANAGI, *Inter. J. Polymer Mater.* **2** (1973) 125.
216. L. E. NIELSEN, *J. Polymer Sci.* **42** (1960) 357.
217. T. NIIKUNI and R. S. PORTER, *J. Mater. Sci.* **9** (1974) 389.
218. T. F. BALLENGER and J. L. WHITE, *J. Appl. Polymer Sci.* **15** (1971) 1949.
219. A. E. EVERAGE Jr. and R. L. BALLMAN, *ibid* **18** (1974) 933.
220. M. T. SHAW, *ibid* **19** (1975) 2811.
221. F. N. COGSWELL, *Polymer Eng. Sci.* **12** (1972) 64.
222. S. MARUYAMA, K. IMADA and M. TAKAYANAGI, *Inter. J. Polymer Mater.* **2** (1973) 105.
223. J. J. BENBOW and P. LAMB, *S.P.E. Trans.* 7 (January, 1963).
224. K. IMADA and M. TAKAYANAGI, *Inter. J. Polymer Mater.* **2** (1973) 89.
225. R. HILL, "The Mathematical Theory of Plasticity" (Oxford Clarendon Press, Oxford, 1950).
226. J. B. SMITH, G. R. DAVIES, G. CAPACCIO and I. M. WARD, *J. Polymer Sci. Phys.* **13** (1975) 2331.
227. K. D. PAE, D. R. MEARES and J. A. SAUER, *J. Polymer Sci.* **B-6** (1968) 733.
228. S. KOJIMA and R. S. PORTER, *J. Appl. Polymer Sci.* (accepted).
229. A. G. KOLBECK and D. R. UHLMANN, *J. Polymer Sci. Phys.* **15** (1977) 27.
230. A. G. GIBSON, I. M. WARD, B. N. COLE and B. PARSONS, *J. Mater. Sci.* **9** (1974) 1193.
231. T. WILLIAMS, *ibid* 8 (1973) 59.
232. H. N. YOON, K. D. PAE and J. A. SAUER, *Polymer Eng. Sci.* **16** (1976) 567.
233. F. J. FUCHS, in "Engineering Solids Under Pressure", edited by H. L. I. D. Pugh (Inst. Mech. Engs., London, 1971).
234. J. M. ALEXANDER, *Mater. Sci. Eng.* **10** (1972) 70.
235. L. A. DAVIS, *Polymer Eng. Sci.* **14** (1974) 641.
236. K. NAKAYAMA and H. KANETSUNA, *Kobunshi Kagaku* **30** (1973) 713.
237. *Idem, Kobunshi Rombunshu* **31** (1974) 256.
238. *Idem, ibid* **31** (1974) 321.
239. S. K. BHAKJA and K. D. PAE, *J. Polymer Sci.* **B-10** (1972) 531.
240. J. R. COLLIER, T. Y. TAITAM, J. NEWCOMBE and N. DINOS, *Polymer Eng. Sci.* **16** (1976) 204.
241. G. S. FARSHYN, V. G. BARANOV and S. YA. FRENKEL, *Vysok. Soedin.* **A12** (1970) 1574.
242. V. G. BARANOV, T. I. VOLKOV, G. S. FARSHYN and S. YA. FRENKEL, *J. Polymer Sci.* **C-30** (1970) 305.
243. V. G. BARANOV, N. I. NYCHKOVSKY, A. SH. GOIKHMAN and M. P. NOSOV, *ibid* **C-38** (1972) 327.
244. T. HASHIMOTO, K. NAGATOSHI, A. TODO and H. KAWAI, *Polymer* **17** (1976) 1063.
245. A. KELLER and M. J. MACHIN, *J. Macromol. Sci.* **B1** (1967) 41.
246. T. T. WANG, H. S. CHEN and T. K. KWEI, *Polymer Letters* 8 (1970) 505.

247. T. K. TWEI, T. T. WANG and H. E. BAIR, *J. Polym. Sci. C* **31** (1970) 87.
248. D. M. BIGG, *Polymer Eng. Sci.* **16** (1976) 725.
249. S. L. CANNON, G. B. McKENNA and W. O. STATTON, *J. Polymer Sci. Macromol. Rev.* **11** (1976) 209.
250. A. W. CHRISTIANSEN, E. BAER and S. V. RACLIFFE, *Phil. Mag.* **24** (1971) 451.
251. J. A. SAUER, *Polymer Eng. Sci.* **17** (1977) 150.
252. M. G. NORTHOLT, *J. Polymer Sci.* **C-38** (1972) 205.
253. G. A. GORDON, *ibid A–2* **9** (1971) 1693.
254. P. LINDENMEYER, *J. Appl. Polymer Sci.* **21** (1977) 821.
255. C. J. FARRELL and A. KELLER, *J. Mater. Sci.* **12** (1977) 966.
256. S. GOGOLEWSKI and A. J. PENNINGS, *Polymer* **18** (1977) 647.
257. *Idem, ibid* **18** (1977) 654.
258. *Idem, ibid* **18** (1977) 660.
259. J. E. STAMHUIS and A. J. PENNINGS, *ibid* **18** (1977) 667.
260. S. G. BURNAY and G. W. GROVES, *J. Mater. Sci.* **12** (1977) 1139.
261. D. P. POPE and A. KELLER, *ibid* **12** (1977) 1105.
262. K. NAKAYAMA and H. KANETSUNA, *ibid* **12** (1977) 1477.
263. A. TRAINOR, R. N. HAWARD and J. N. HAY, *J. Polymer Sci. -Phys.* **15** (1977) 1077.
264. P. J. BARHAM and R. G. C. ARRIDGE, *ibid* **15** (1977) 1177.

Received 11 February and accepted 27 May 1977.